Accepted Manuscript

Spatial and Temporal Variability of Groundwater Recharge in Geba Basin, Northern Ethiopia

Alemu Yenehun, Kristine Walraevens, Okke Batelaan

PII:	S1464-343X(17)30262-5
DOI:	10.1016/j.jafrearsci.2017.06.006
Reference:	AES 2929
To appear in:	*Journal of African Earth Sciences*
Received Date:	06 December 2016
Revised Date:	17 June 2017
Accepted Date:	19 June 2017

Please cite this article as: Alemu Yenehun, Kristine Walraevens, Okke Batelaan, Spatial and Temporal Variability of Groundwater Recharge in Geba Basin, Northern Ethiopia, *Journal of African Earth Sciences* (2017), doi: 10.1016/j.jafrearsci.2017.06.006

Spatial and Temporal Variability of Groundwater Recharge in Geba Basin, Northern Ethiopia

Alemu Yenehun[a,b], Kristine Walraevens[c], Okke Batelaan[d]

[a]Department of Hydrology and Hydraulic Engineering, Vrije Universiteit Brussel, Pleinlaan 2, 1050 Brussels, Belgium

[b]Department of Earth Science, Bahir Dar University, P.O. Box 79, Bahir Dar, Ethiopia

[c]Laboratory for Applied Geology and Hydrogeology, Department of Geology, Ghent University, Krijgslaan 281-S8, 9000 Gent, Belgium

[d]School of the Environment, Flinders University ,GPO Box 2100, Adelaide SA 5001, Australia

Abstract

WetSpa, a physically based, spatially distributed watershed model, has been used to study the spatial and temporal variation of recharge in the Geba basin, Northern Ethiopia. The model covers an area of about 4, 249 km^2 and integrates elevation, soil and land-use data, hydrometeorological and river discharge data. The Geba basin has a highly variable topography ranging from 1000 to 3,280 m with an average slope of 12.9%. The area is characterized by a distinct wet and long dry season with a mean annual precipitation of 681 mm and temperatures ranging between 6.5°C and 32°C. The model was simulated on daily basis for nearly four years (January 1, 2000 to December 18, 2003). It resulted in a good agreement between measured and simulated streamflow hydrographs with Nash-Sutcliffe efficiency of almost 70% and 85% for, respectively, the calibration and validation. The water balance terms show very strong spatial and temporal variability, about 3.8% of the total precipitation is intercepted by the plant canopy; 87.5% infiltrates into the soil (of which 13% percolates, 2.7% flows laterally off and 84.2% evapotranspired from the root zone), and 7.2% is surface runoff. The mean annual recharge

varies from about 45 mm (2003) to 208 mm (2001), with average of 98.6 mm/yr. On monthly basis, August has the maximum (73 mm) and December the lowest (0.1 mm) recharge. The mean annual groundwater recharge spatially varies from 0 to 371 mm; mainly controlled by the distribution of rainfall amount, followed by soil and land-use, and to a certain extent, slope. About 21% of Geba has a recharge larger than 120 mm and 1% less than 5 mm.

Key Words: WetSpa; Geba catchment; Groundwater recharge; Water balance; Northern Ethiopia

1. Introduction

Rainfall in Africa is highly variable. About 95% of the annual rainfall varies between plus or minus 20% to 40% from the average value (Carter and Parker, 2009). Highest differences occur during the wettest months when the contribution of net precipitation (i.e. the share of precipitation that produces runoff and groundwater recharge) to the land surface is highest (Taylor et al., 2009). Rainfall is the main available water for both agricultural and domestic uses in Ethiopia. In the Geba catchment, which is characteristic for the Northern part of the country, the rainfall is low, and evapotranspiration is high. Moreover, rainfall is highly variable and uneven in time and space (Eyasu, 2005; Hadgu et al., 2013). The wet season is limited to less than three months of the summer season during which the vegetation cover dwindles, surface runoff is short-lived and rivers are ephemeral or carry little water. Similarly, recharge to the groundwater is limited and sustainable groundwater abstraction is nearly impossible. Although existing regional studies (Seleshi and Zanke, 2004) and meteorological records in the Geba basin show that the long term total rainfall trend has remained more or less constant since the 1950s, the high spatial and temporal variation together with recurrent drought causes farmers in the basin to be continuously impoverished. In general, Geba River catchment is a major upstream

catchment of the Blue Nile Basin, which is particularly affected by low and high viability of erratic rainfall. It is representative for a semi-arid mountainous catchment where people's livelihood is strongly affected by the climatic conditions. Hence, it is becoming clear that food self-sufficiency can only be attained by adopting a strategy which encourages conjunctive groundwater and surface water use and management. Understanding the availability, distribution and sustainability of groundwater resources for supplementary irrigation can help to alleviate the water stress, thereby improving crop production.

Groundwater is type of renewable water resources exploited and used to address the rapidly increasing domestic and agricultural water requirements. To quantify the current ground water storage and to predict the potential groundwater availability and sustainability, quantifying recharge is a primary task. Groundwater recharge is defined as the entry of water into the saturated zone made available at the water table surface (Freeze, 1969). It is thus a prerequisite for efficient and sustainable groundwater resource management and development (De Vries and Simmers, 2002).

Distinct wet and dry seasons are the climatic characteristics of the Tigray (Northern Ethiopia) highlands. Thus groundwater recharge is absent during the dry season except for shallow aquifers downstream of many micro-dams, as observed by Nedaw and Walraevens (2009) for Tsenkanet and Rubafeleg micro-dams, where recharging prolongs far into the dry season, and for confined aquifers with remote recharge zone. During the dry season, groundwater level lowers dramatically and the mountain slope phreatic aquifer drains away nearly completely in the upstream section, by the strong gravity-force, for sustaining discharge downstream, whereby the rate decreases through time (Walraevens et al., 2009).

Different methods have been applied to estimate groundwater recharge (Healy and Cook, 2002). Important factors taken in to considerations in choosing a technique include spatio-temporal scales, range, and reliability of estimates (Scanlon et al., 2002). The need for recharge estimates is growing in the research community. Thus, the community is forced to develop approaches for building a more thorough understanding of recharge, more comprehensive methods for delineating recharge zones and quantifying recharge rates with lower uncertainties which increase confidence in recharge estimates (Scanlon et al., 2002).

The distribution of recharge with time and space in this century is expected to be greatly altered due to changes in land-use and climate (Bouraoui et al., 1999). These changes may have consequences as recharge is the one on which groundwater depends for its sustainability. If the sustainability of this natural resource is disturbed, shortage of drinking water and disturbance of stream ecosystems especially during the dry season will occur and will greatly affect human life. Even though the importance of recharge is well known in both the research and professional community, its spatial and temporal distribution is not generally well understood. Many hydrological modeling studies ignore time and space variations in recharge rates, either due to few measurements of critical parameters are available, or existing modeling methods are not adequate to accurately evaluate these variations with required scale.

In this study, the spatial and temporal variation and amount of recharge and other water balance components are simulated using Westpa. Westpa is a physically based, distributed hydrological model developed for predicting the Water and Energy Transfer between Soil, Plants and Atmosphere on regional or basin scale at daily time-step. It was originally developed at the Vie Universities Brussels, Belgium by Wang et al. (1996) and adapted by Liu and De Smedt (2004). The model has been extensively used in surface water studies (e.g., Chormański and

Batelaan, 2011; Gebremeskel et al., 2005; Imani et al., 2016; Karamage et al., 2017; Liu et al., 2002; Rwetabula et al., 2007; Safari et al., 2012; Safari and De Smedt, 2014, 2008). It has also been applied for recharge estimation (e.g., Adem and Batelaan, 2006; Dams et al., 2012; Woldeamlak et al., 2007).

1.1. Previous groundwater recharge studies in Geba basin and the need for a new study

Gebreyohannes et al. (2013) assessed groundwater recharge and other water balance components for the Geba basin, using a spatially distributed water balance model called WetSpass. The WetSpass model requires two types of input data, i.e. GIS grid maps and parameter tables (Batelaan and De Smedt, 2001). The grid maps consist of slope angle, land-use, soil texture, groundwater depth, and seasonal meteorological maps of precipitation, potential evapotranspiration, temperature and wind speed. The WetSpa model, applied in this study, requires also grid maps of slope, land-use, and soil texture but additionally time series of rainfall, potential evapotranspiration, and river discharge. However, different from WetSpass, WetSpa simulates hydrological processes on a daily (hourly) basis while WetSpass calculates seasonal water balance and focuses only on simulation of spatial patterns. Hence, in this study daily rainfall, PET and river discharge (at the main river outlet) are used to run, calibrate and validate the model for four years (2000 to 2003). Applying WetSpa, in this study, will present the advantage of outputs of both the spatial and temporal variations of the hydrological states and fluxes in the basin. Furthermore, since the study of Gebreyohannes et al. (2013), the land-use has changed, noticeable areas (in the north and central part) are rehabilitated and vegetation coverage increased while some are further degraded. Gebreyohannes et al. (2013) used Landsat ETM+ images taken in January, 2000 in their land-use preparation while Landsat ETM+ images of 2007

were applied in this paper. The intensive community based land and water conservation campaigns applied in the late 1990s and early 2000s, coordinated and funded by the Regional Government, flourished and brought results in changing the bare soil land cover percentage in to vegetation containing land-use types like open and closed shrub land. However, part of the forest land-use type in the previous study is regarded as closed shrub land in our classification (the important changes are shown in table 1). As a result the new land-use map would bring changes of groundwater recharge and other water balance components. High rate of land-use change from degraded (bare land) to vegetated was also obtained by other researchers. Fenta et al. (2017) assessed land-use/land cover change in the periods: 1990-2000, and 2000-2012 on Agulae catchment, tributary of Geba basin, having areal coverage 442 km^2 and located in the central part of the basin (Fig.1). According to them, significant changes were observed for shrub land and forest cover which increase by about 18 and10 km^2 in the period 1990–2000; and then further increased by about 4 and 6 km^2, respectively, during 2000–2012. By contrast, bare land was subjected to considerable reductions by about 23 and 13 km^2 in the periods 1990–2000 and 2000–2012, respectively. Similar results of vegetation coverage increment were also noted by Alemayehu et al. (2009) and Kassie et al. (2015) for the same Agulae catchment and for the whole of eastern Tigray, to which our study basin belongs. In addition, the new study used daily recorded meteorological variables (rainfall, minimum and maximum temperature) from seven meteorological stations whereas Gebreyohannes et al. (2013) used the long term average seasonal values of the variables from only four stations. Thus the output of the WetSpass recharge and other balance components were long term seasonal averages and hence, daily comparisons and trend assessment were impossible. However, in this study, it is aimed to

investigate the hydrological response of the basin, due to changes of physical aspects such as land-use and meteorological variables (rainfall and PET), over long and short time periods.

Table 1 Land-use change comparisons between the study and the previous by Gebreyohannes et al. (2013)

Land use types	Areal coverage in % in this study	Areal coverage in % during Gebreyohannes et al.(2013) study
Agricultural Land (grazing or grass and Cropland together)	51	50
Shrub Land (both open and closed)	34	20
Bare land	10	20
All the rest (urban, forest, and water)	5	10

Tesfagiorgis et al. (2011) applied the MODFLOW groundwater flow model to see the movement and distribution of groundwater in the whole Geba basin. They applied the model with limited data availability and simplified the hydrogeology to a single layered semi-confined groundwater aquifer system and optimized the transmissivity of the different geological units. They concluded that 30,000 m^3/d of groundwater can be abstracted in the basin in a sustainable way. Walraevens et al. (2009) quantified the groundwater recharge on a daily basis using a combination of a runoff estimation model, based on the US Soil Conservation Service method, and a soil moisture balance model, on a very small (2 km^2) part of the Zenako-Argaka catchment, sub-catchment of Geba, located east of the town of Hagere-Selam. The study is performed on a local scale but can be assumed to represent the sloped upper phreatic aquifer of the Trap basaltic formation which topographically represents most part of the basin. According to their study, the annual groundwater recharge varies from 110 mm to 334 mm for the years 1995 to 2006.

In addition, Walraevens et al. (2015) determined the water balance of Mendae plain located in Abraha Atsbeha area, in a small part of the Suluh River catchment, which is one of the major tributaries of the Geba basin (Fig. 1). In this study, the sustainability of pumping (from

shallow hand dug wells mainly for irrigation) and the effectiveness of the constructed water harvesting structures (ponds) were evaluated through identification and quantification of the groundwater balance components. As part of the balance components, the recharge is quantified in a diffuse manner using the soil moisture balance (on monthly basis) and chloride mass balance methods. Accordingly, the grass land and the irrigated land have monthly average recharge ranging from 0 to 300 mm and the bare soil has an annual average recharge of 20 mm. Gebreyohannes et al. (2017) ran the 3D numerical groundwater flow model program MODFLOW-2000 using simulated recharge obtained by Gebreyohannes et al. (2013) According to their work they concluded that the precipitation is the only source of recharge to the basin which is about 5.14×10^5 m^3/d in total. About the same amount of groundwater drains out of the system through springs and base flow to streams and rivers. A very small part, i.e. about 2.2×10^3 m^3/d is extracted through pumping wells.

1.2. Objectives of the Study

The overall aim of this study is to provide information on the rates of groundwater recharge and other water balance components, and how they are spatially distributed and change with time. It tries to identify the key recharge-controlling basin characteristics and meteorological variables with their degree of influence. It also aims on analyze and justifiy the interrelationship of groundwater recharge with other hydrological processes throughout the year. Furthermore, understanding the relationship and sensitivity of recharge and other hydrological components with landcover/land-use, and hence predicting the human impact on groundwater resources is also addressed in the study.

1.3. General Overview of the Study Area

1.3.1. Location, Topography and Drainage System

The Geba catchment is situated in Tigray Regional State, Northern Ethiopia. It is bounded between latitudes of 13˚16' and 14˚16' North and longitudes 38˚38' and 39˚49' East.

The Geba basin covers an area characterized by rugged terrain, with topography ranging from about 1000 to 3,280 m (Fig.1). The total areal coverage of the Geba river basin is about 5,150 km^2. Because of lack of river discharge data (one of basic data in the WetSpa model) at the main basin outlet, the catchment's lower part, with some small tributaries to the main Geba river basin is excluded. As a result, our study area has coverage of 4,249 km^2.

Geomorphologically, the Geba river basin is characterized by steep volcanic mountains with sharp cliffs and plateaus of sandstones in the north, deep gorges and cliffs of limestone in the center, and ragged metamorphic terrain in the southwest. The fault-controlled Mekelle, Wukro and Senkata areas, and the Atsbi horst, are the major plains of the Geba basin.

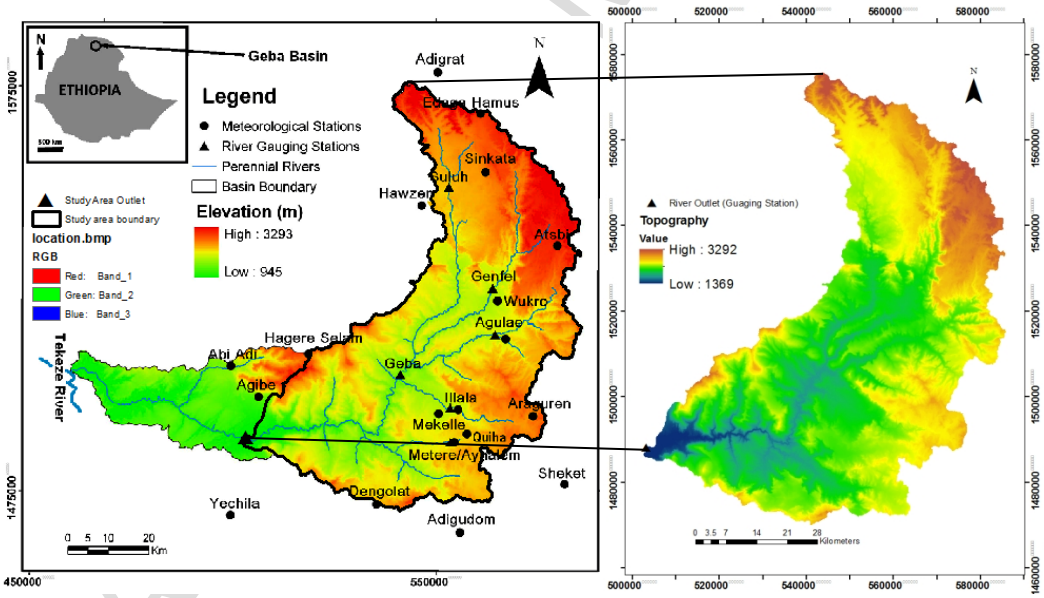

Fig. 1.Location map of the main Geba basin from Gebreyohannes et al. (2013) **and the study area(part of Geba basin) with meteorological and gauging stations**

The Geba basin is a major tributary of the Tekeze River which is one of the main tributaries of the Blue Nile. The Tekeze River joins the Nile River in Atbara, Sudan. Suluh, Genfel and Agulae Rivers are the major tributaries of Geba River basin. The drainage system of the Geba basin can generally be described as dendritic with some significant influence of major structures like folds and faults. The Geba River and its tributaries exhibit deep gorges especially in soft formations, like shale rock formation in the Mekelle sedimentary basin of Geba. The Geba River flows southwards in the northern part of the basin, and turns to the west in the southwest. The major tributaries of the river are perennial, with very low discharges, though the region is characterized by short-lived flash floods taking place during or shortly after rainfall event.

1.3.2. Climate and Vegetation

The Geba basin has a mean annual rainfall of about 681 mm and a mean annual minimum of 544 mm and maximum of 912 mm (from the data taken of the seven meteorological stations used in this study). The rainfall is found highly variable and inconsistent in time and space, in agreement with Hadgu et al. (2013) and Fenta et al. (2017), for northern Ethiopian, and Agulae catchment, respectively. Much of the annual rainfall occurs in the short wet season (from beginning of June to September). The rest of the years are generally dry, except for spring when small amounts of rainfall occur in some parts of the basin. Temperature varies from a mean minimum of 6.5°C in the highlands, to a mean maximum of 32 °C in the lowlands. The forest cover of the basin is very minimal. Unpublished report works showed much of the area in the past was forested, and subsequently later deforested. Except for the more protected areas around churches and some closed areas, there is hardly any trace of large indigenous trees. Recently, some initiatives to create closure areas to rehabilitate parts of the environment have shown

encouraging results (Alemayehu et al., 2009; Fenta et al., 2017; Kassie et al., 2015). These closure areas are populated by bushes and shrubs like acacia rarely mixed with eucalyptus and other plantations. More importantly, the closed areas are covered with grass, which protects the soil from erosion and enhances infiltration.

1.3.3. Geology

According to Gebreyohannes et al. (2010), the geology of Geba basin (the major part of which is included in this study) comprises lithological units such as Quaternary alluvial sediments; Paleogene period volcanic rocks; Mesozoic and Paleozoic sedimentary rock types; Precambrian metamorphic and intrusive rocks; and post-Mesozoic dolerite dikes and sills. The Mesozoic sedimentary rocks consist of upper (regionally called Ambaradom) sandstone, Agulae shale formation (consisting of dominantly shale, limestone, some gypsum), Antalo limestone formation (dominated by limestone but with shale and marl intercalations), lower (Adigrat) sandstone formation, while the white Enticho sandstone and Edaga Arbi tillite corresponds to the Paleozoic era. Granite dominated intrusives, meta sediments (slate, phyllite, meta-limestone, meta-dolomite, meta-greywacke, and meta-conglomerate), and meta-volcanics (meta-volcanoclasts) aged back to Precambrian are the rock varieties in the metamorphic terrain of the study area. The Wukro, the Chelekot and Mekelle main faults, and the Negash geosyclinal fold are the major and regional geological structures though the local scale joints and faults are many in number and variable in character such as displacement, sense of movement, spacing, aperture continuity, fillings, etc.

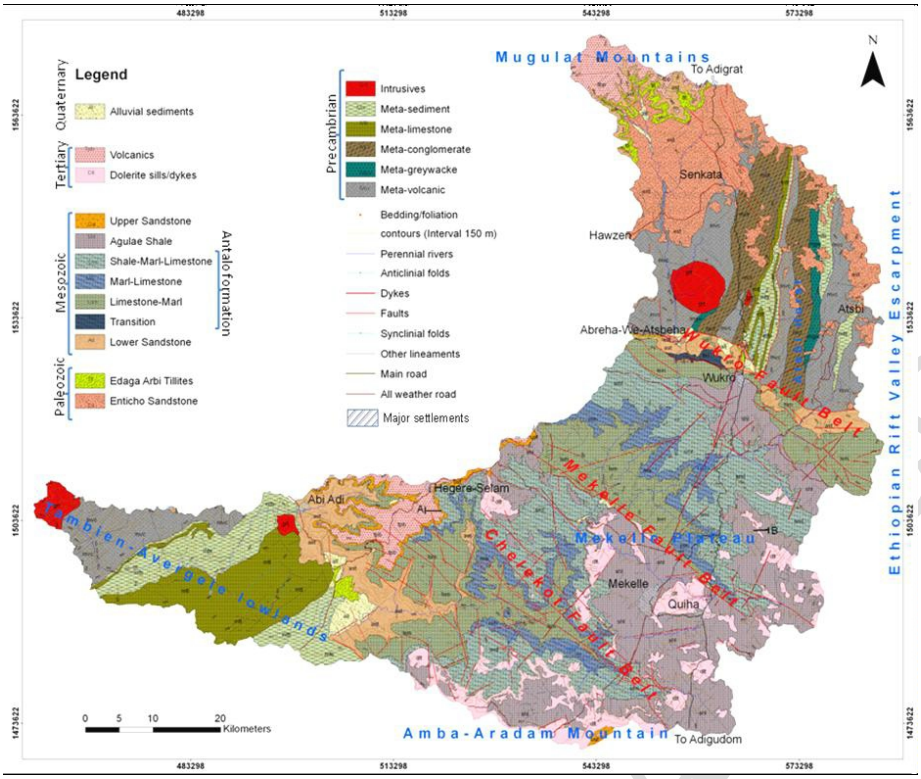

Fig. 2. Geological map of the whole Geba basin after Gebreyohannes et al. (2010) **of which our study area (Fig.1) makes the major part**

1.3.4. Land-use and Soil type

The land-use map (Fig. 3) is prepared in this study by using cloud free Landsat ETM+ satellite images (taken on January 27 and February 5, 2007), ground truth data, and Google Earth images with image classification functions of ILWIS GIS software. Initially eleven land-use classes were identified which later were reclassified to eight classes (mixed forest, closed shrubs, open shrubs, grassland, cropland, urban, bareland and water). Grassland is the dominant type of land-use which covers about 27.5% of the total study area while water bodies only account for 1.1%. The closed shrub covers 21.0%, open shrub 12.6%, cropland 23.5%, 9.7% bare land, 3.2% urban and 1.4% of the study area is covered by mixed forest.

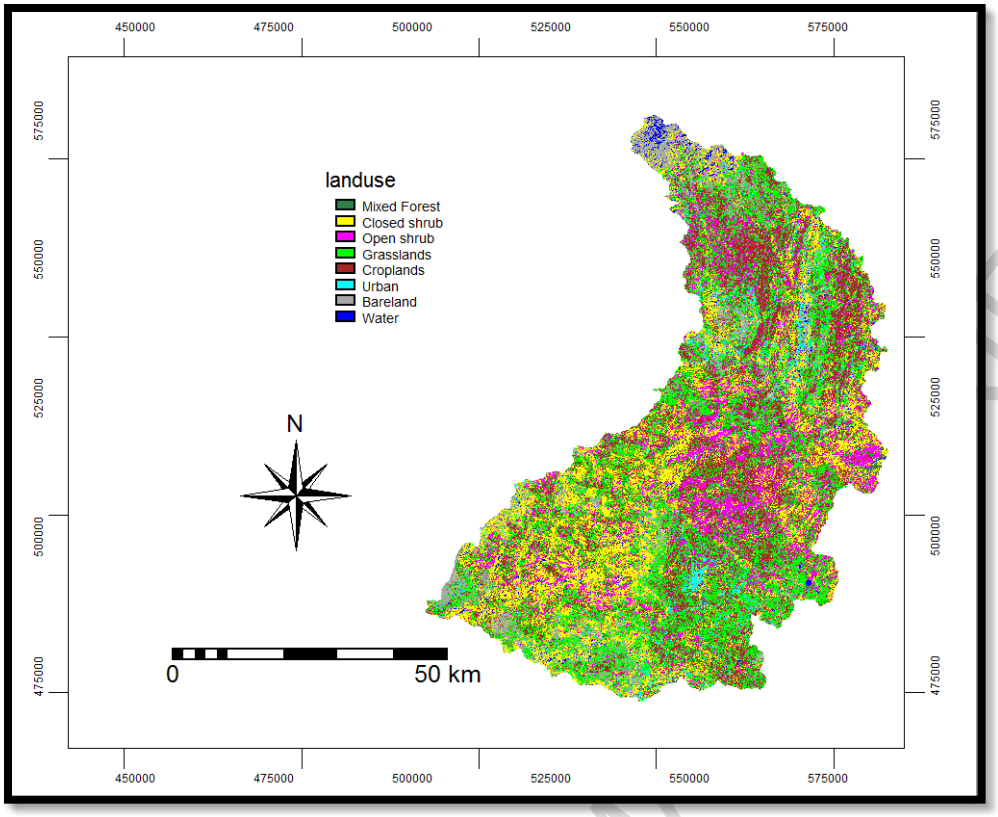

Fig. 3. Land-use map of the study area

The soil map of the study area is adapted from Gebreyohannes et al. (2013) where detail preparation procedure is mentioned in the article. The map (Fig.) shows that clay loam and clay together make up 72.8% of the surface area of the study basin with the rest being sandy clay loam (16.7%), sandy loam (4%), sand (4.2%), and loam (2.4%).

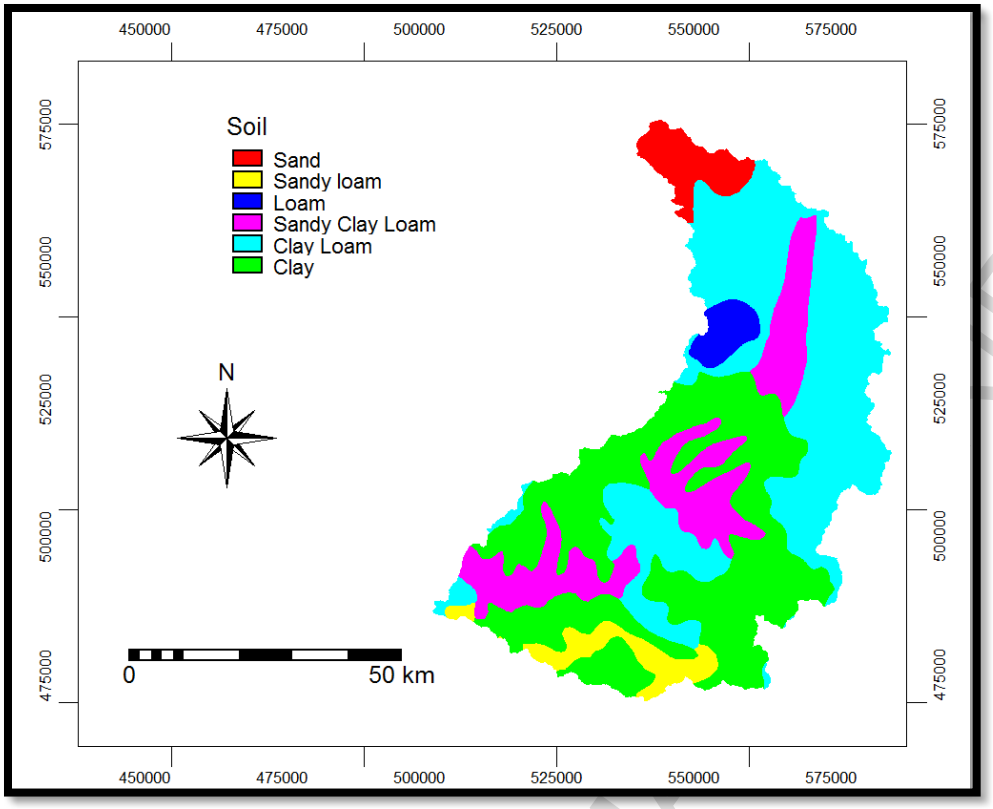

Fig. 4. Soil map of the study basin after Gebreyohannes et al. (2013)

2. Methodology

Fig. 5 shows a flow chart of the modeling procedure. The spatial data (land-use, topography, and soil) and hydro(meteoro)logical time series data (precipitation, PET and river discharge) are the basic data in the applied model. The hydro(meteoro)logical data are equally split into data for calibration and validation. In the ArcView GIS the DEM is preprocessed (filling the sinks) before parameters are derived from the surface topography. The rainfall and the PET daily time series data are prepared for each meteorological station for the whole simulation period. Following data preparation, the WetSpa model was run using the default values of its global parameters (Table 2). Using manual and automatic calibration (with PEST), the model was rerun several times by adjusting the values of the eleven parameters while each

time checking the statistical efficiency model performance indicators (Table 3). After calibration was achieved, the model efficiency was also tested with the independent validation hydro(meteoro)logical data series. The following sections explain detailed methods followed in this paper.

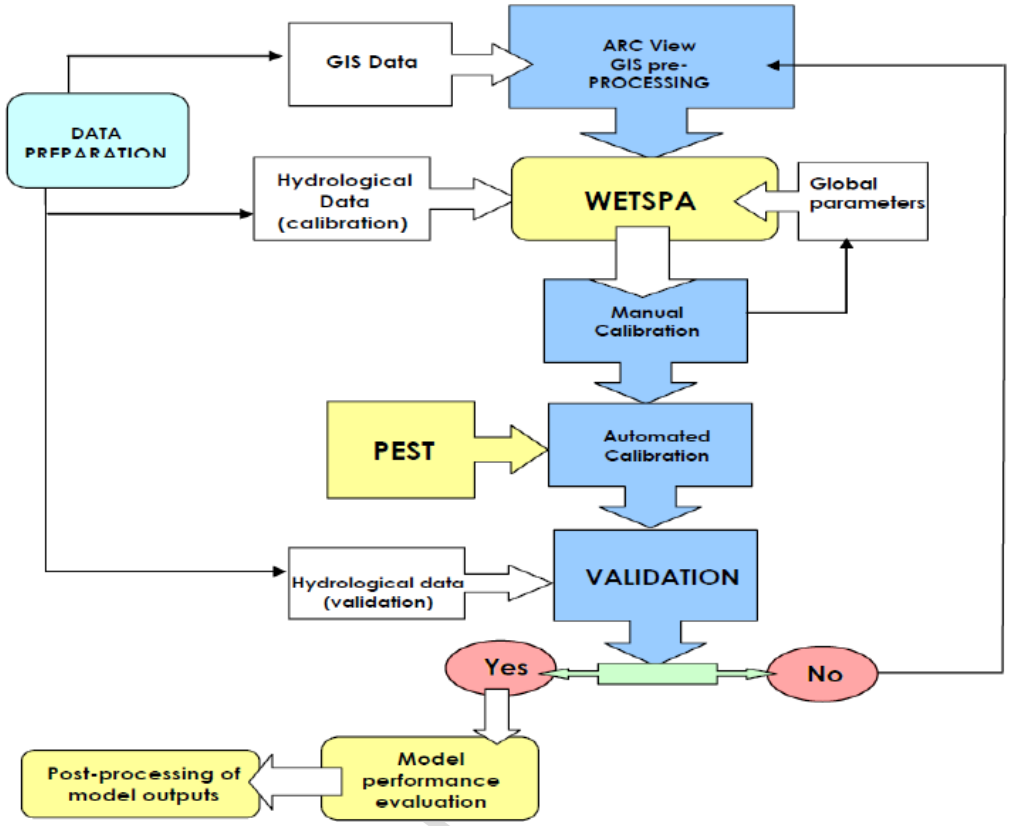

Fig.5. Flow chart showing the general methodology

2.3. Grid Data Preparation and Parameter Derivation

Grid maps from the 90 m by 90 m DEM, the land-use map and the soil hydraulic properties from the soil map of the basin have been prepared.

For flow direction and then accumulated flow are depicted accurately if the data set is free of sinks (Liu and De Smedt, 2004). Thus the DEM was made depression-less using the fill sinks function so that drainage would occur throughout the basin. The spatial model parameters

necessary for WetSpa were then created using the functions in ArcView. Flow direction and accumulation grid maps are prepared from the filled topographic map, based on the flow path of steepest descent. The vector stream network is extracted from the result of flow accumulation using a threshold cells value of 100. This means that cells receiving a flow from more than 100 cells are considered stream cells.

Shreve's method (Tarboton et al., 1991) was used to derive the stream order grid which is used for assigning the channel's Manning coefficient n by taking the Flow Direction and Stream Network grid themes. The general slope in percentage was derived from the DEM. The slope along a stream or river needs extra stream network information for their preparation. As a result, Extracted stream network and the general slope were used to calculate the channel slopes. This was to avoid the disturbance of channel slopes. By overlying the general slope grid, with the channel slope grid, the final slope grid is obtained.

Sub-catchments are derived from the filled DEM using 1000 as a cell threshold value. 272 sub-catchments are identified with an average sub-catchment area of 1.56 km^2; with 0.0081 km^2 and 11.68 km^2 as minimum and maximum areas respectively. These derived sub-catchments are used to simulate the groundwater balance in the distributed model.

The land-use based parameters (root depth, interception capacity, and the Manning's coefficient), and the WetSpa model parameters of potential runoff coefficient and depression storage capacity have been derived from previously created maps of slope, land-use and soil types. The soil hydraulic properties such as hydraulic conductivity, porosity, field capacity, residual moisture content, pore distribution index and wilting point were derived from the soil map.

2.4. Flow Routing Parameters

The flow routing variables of flow velocity and average travel time from cells to the basin outlet are calculated in the view 'Routing Parameter'. Manning's coefficient, hydraulic radius and slope grids are used to create a flow velocity grid using the velocity function of the model. The default flow velocity limits of 3.0m/s for upper and 0.005 m/s for lower were applied. Though the slope of the area is high, the average flow velocities are fairly slow, which is due to the very low hydraulic radius (most part is between 0.005 to 0.0311 m), and the relatively high Manning's roughness coefficient of the catchment. The weighted 'FLOWLENGTH' routine of the model is applied to create flow travel time in hours from each cell to the basin outlet.

2.5. Time Series Data Preparation

The WetSpa reads input data from four input files: precipitation, potential evapotranspiration, average temperature and river discharge. In case of snowfall, average temperature data are required by WetSpa, because the melting snow affects the hydrological system of an area. However, there is no any snowfall record in this study catchment; as a result the preparation of average temperature point data of the meteorological stations was unnecessary, in this study, though the daily minimum and maximum temperature data are used in PET calculation. In general, there are thirteen meteorological stations in the Geba catchment. Among these, only seven (Mekelle-Quiha, Wukro, Sinkata, Adigrat, Hager-Selam, AbiAdi, and Hawzen) had complete rainfall, minimum and maximum temperature. Among them, it was only three stations (Mekelle-Quiha, Sinkata, and Adigrat) that had daily sunshine hours, wind speed and relative humidity data while the other four had only records of rainfall, minimum and maximum temperature.

2.5.1. Rainfall Data Preparation

The daily rainfall data for the four years starting from January 1, 2000 to December 18, 2003 are taken from the National Meteorological Service Agency of Ethiopia (Mekelle branch). The data for the period were complete except very few gaps, where daily average values of same days from the months of preceding and following years had been taken. Rainfall data for the seven meteorological stations were prepared.

2.5.2. *Potential Evapotranspiration*

The daily potential evapotranspiration for the simulation period (January, 2000 to December, 2003) was prepared using data of minimum and maximum temperature, relative humidity, radiation, sunshine hours, and wind speed by applying the Daily ETo Penman Monteith method (Allen et al., 1998) using the CROPWAT 8 software (Smith 1992, 1994, 1996). The daily recordings of the minimum and maximum temperature for the whole simulation period in the seven meteorological stations were complete except some gaps for which average values of preceding and following years of corresponding days had been taken. However, values for humidity, wind speed and sunshine hours are only available for Mekelle-Quiha, Sinkata and Adigrat stations, with daily gaps and no recorded values for the whole year of 2000. For such cases the software calculates a value using the maximum and minimum temperature and location information alone. The daily PET values for the seven stations (three with more or less recorded values of relative humidity, sunshine hours and wind speed and the remaining four from maximum and minimum temperature alone) are prepared in this manner. The sensitivity of the PET for the relative humidity, sunshine hours and wind speed was checked for the stations with these data during data preparation. It was found that the calculated PET values using minimum and maximum temperatures alone and those calculated with complete data sets are similar,

showing the less sensitive character of the PET for these meteorological variables in this particular study area.

2.5.3. River Discharge Data

There are daily river discharge data available at the Geba catchment (part included in this study) outlet for the whole model simulation period (2000-2003). River discharge recordings starting already from March 26, 1998 were available at the measuring point. However, daily PET data until December 30, 1999 are not available due to the absence of recorded minimum and maximum temperature and other meteorological variables. On the other hand, from December 18, 2003 to December 31, 2006, the daily rainfall and the PET data are calculated but there are no recorded river discharge data at the measuring point. The WetSpa model runs only if the time series data have the same corresponding time period. As a result, the daily time series data from March 26, 1998 to December 30, 1999 and from December 18, 2003 to December 31, 2006 are not used because of the absence of PET and discharge data respectively.

2.6. Thiessen Polygon

The rainfall and PET data are tabular data gathered from these seven meteorological stations among which three are inside the catchment (Mekelle-Quiha, Wukro, Sinkata), two at the boundary (Hagere-Selam and Hawzen) and two nearby surrounding the catchment (Abi Adi and Adigrat). The Thiessen polygon grids for both precipitation and PET were created using the Thiessen polygon extension. Precipitation and PET are point measurements; therefore Thiessen polygon method was applied to interpolate the distribution of precipitation and PET over the area. There is no snowfall record in the study basin; as a result the preparation of temperature Thiessen polygon was omitted in this study.

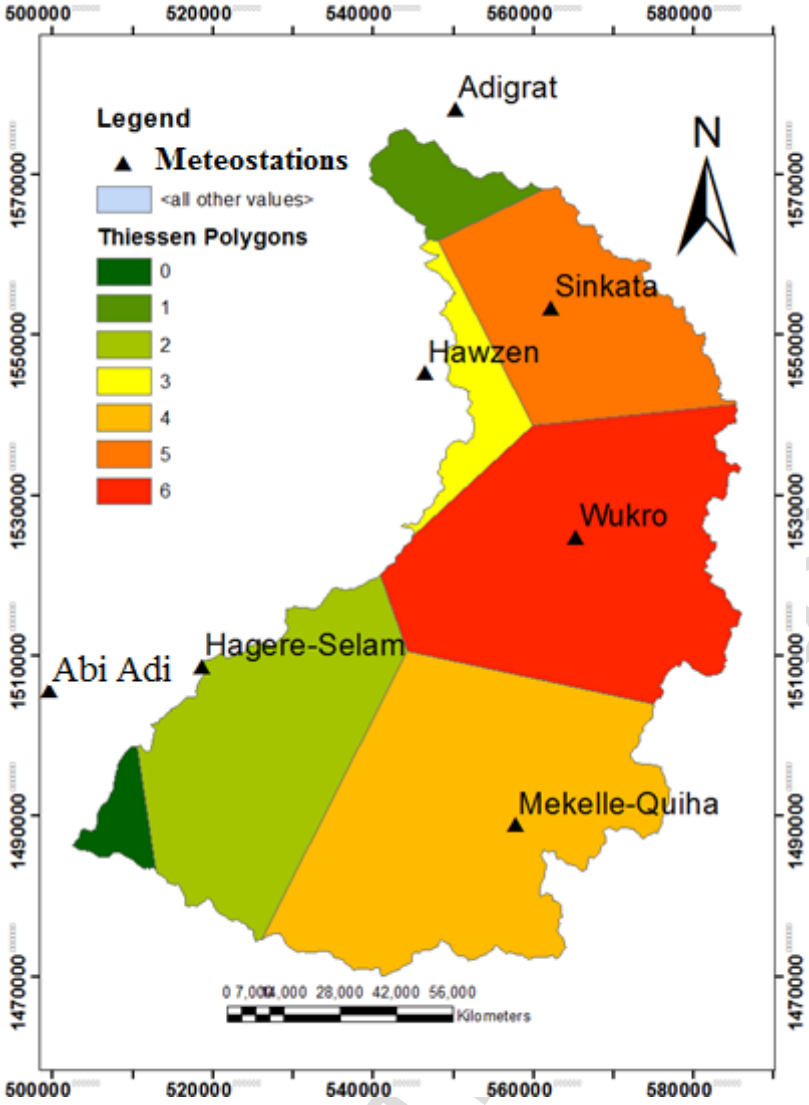

Fig. 6. Thiessen polygon for both rainfall and PET estimation.

2.7. Model Calibration and Validation

The data series with discharge recordings was divided into two parts (for model calibration and validation). Model calibration was performed for the period between 1/1/2000 to 26/12/2001 and validation for the period 27/12/2001 to 18/12/2003. The model was first calibrated manually to set up the parameters for the automated calibration by using the model independent parameter estimator, PEST software (Parameter Estimation module), in which the development and latter integration to the WetSpa model was done by Doherty (2010) and Liu et

al. (2005) respectively. The calibration is mainly taken place for the global model parameters, whereas the spatial parameters are maintained (Doherty, 2010). After running PEST, the model was then run for the complete time series (January, 2000 to December, 2003), and consequently the final spatial and temporal water balance components are produced as an output.

3. Results and Discussion

3.1. Grid and flow routing parameter maps

The study area is generally regarded as steeply sloped. It has a slope of 12.9% on average with a minimum of 0.01% and a maximum of 207% which illustrates the highly variable topographic scene of the area. As shown in Fig. 7, thirty one percent of the area has a slope of between 0.01% and 5%. Besides, 23%, 15%, 10%, 11%, 8%, and 2% of the area are covered by 5-10%, 10-15%, 15-20%, 20-30%, 30-50%, and 50-207% slope ranges, respectively.

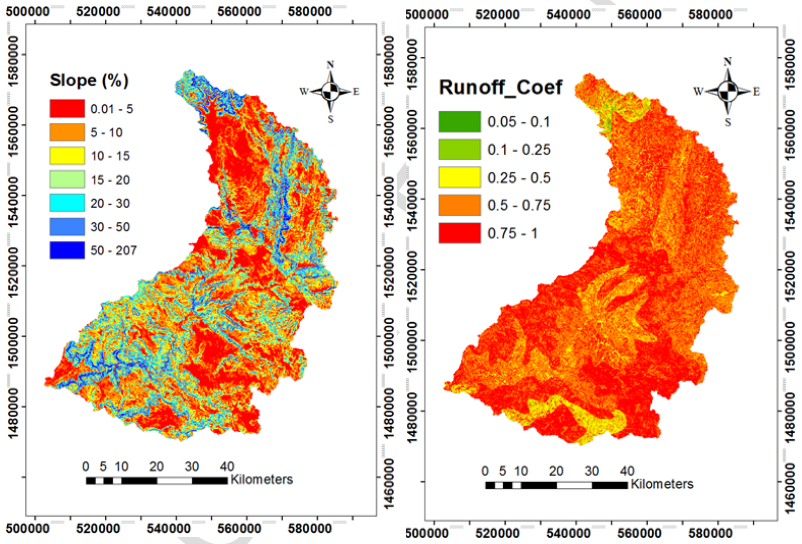

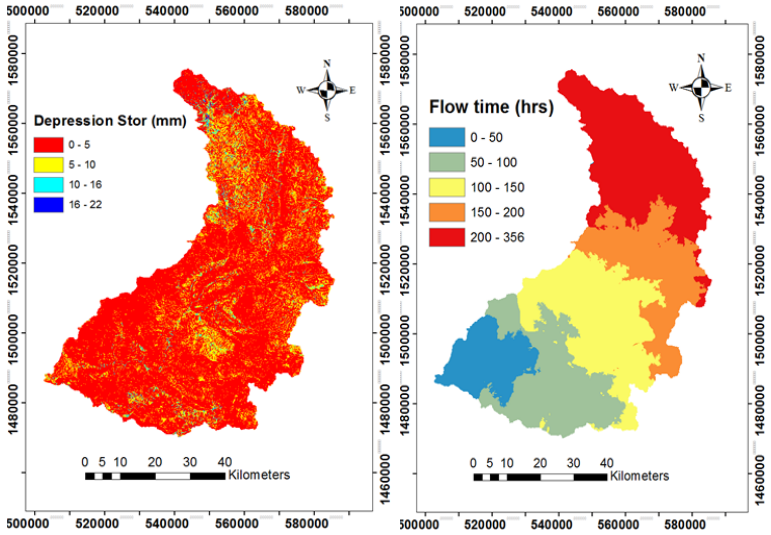

Fig. 7. Slope, runoff coefficient, depression storage and flow time maps of Geba basin

The slope (Fig. 7), land-use (Fig. 3), and soil (Fig.4), play an important role in determining the potential runoff coefficient. A steeply sloped urban or bare land with clay or clay loam soil type has the highest potential runoff coefficient, whereas sandy loam or sandy soil of forest land-use has relatively small value (Fig.7). Especially relatively flat, sandy or sandy loam forest land reaches as low as 0.051 and sandy clay loam up to 0.156. However, steep, clayey, bare or water land-use land reaches up to a value of 0.9.In the other hand, as the catchment area gets larger, the runoff decreases (Brown et al., 1999). In a similar way, Singh and Woolhiser (2002) found out increasing of runoff coefficient with decreasing grid size. In this study, grid size is 90 m by 90 m which is large. The calculated average potential runoff coefficient for the entire catchment is about 0.7 which is relatively high though the catchment is large. This fact can be attributed to the relative steepness and the dominant clay soil type. However, contrary to the potential, the actual runoff coefficient is much lower for reasons mentioned in the result and discussion section.

Depression storage capacity in the Geba catchment (Fig. 7), mainly depends on land-use and slope. Sloping urban, water or bare land has very small depression storage capacity of about 0 to 2.415 and a forested flat area has up to 21.7. The average value for the whole catchment is about 1.4 which is quite small.

The calculated flow travel time (hours) from each cell to the catchment outlet is shown in Fig. 7. The concentration time, defined as the time it takes for water from the furthest point to reach the outlet of the catchment is around 356 hours or 14.8 days. The mean travel time for the entire catchment and the maximum flow length are 6.6 days and 166.6 km respectively.

3.2. Model Performance Indicators and Hydrographs

3.2.1. Global Parameters Adjustment

The calibrated global parameters are shown in Table 2. As there is no snow in the study catchment, the parameters T0, K_snow and K_rain are set to negative values, e.g. –1.0, and the temperature input dataset totally is omitted (Liu and De Smedt, 2004).

Table 2 Calibrated global parameters.

Symbol	Unit	Values
Ki	-	1.266
Kg	-	0.00036
K_ss	-	1.0423
K_ep	d^{-1}	1.6292
G0	mm	13.2
G_max	mm	334.7
T0	-	-1.00
K_snow	mmd^{-1}	-1.000
K_rain	°C	-1.0000
K_run	$mm°C^{-1}d^{-1}$	8.5128
P_max	$mm°C^{-1}d^{-1}$	152.7

Ki: interflow scaling factor for computation
Kg: Groundwater recession coefficient.
K_ss: relative moisture content for setting up the initial soil moisture constant
K_ep: plant coefficient for estimating the actual potential evapotranspiration.
Go: initial groundwater storage in water depth (mm)
G_max: maximum groundwater storage in water depth (mm)
T0: base temperature for calculating snowmelt (°C)
K_snow: degree-day coefficient for calculating snowmelt (mm/°C/day).
K_rain: rainfall degree-day coefficient for estimating snowmelt (mm/mm/°C/day)
K_run: surface runoff exponent for a near zero rainfall intensity.
P_max: threshold rainfall intensity in mm/day or mm/hr.

3.2.2. Model Performance Indicators

Model performance can be verified by visual interpretation of the flow hydrographs as well as by statistical criteria (Gebremeskel et al., 2004). These statistical criteria are shown in Table 3.

Table 3 shows values of the model performance indicators for manual calibration, for calibration using PEST and for validation. In general, better Nash-Sutcliffe (NS) and Model Bias results have been obtained by using PEST than for the manual calibration as shown in the table below. However, NS for evaluating the ability of reproducing low flows was lowered for PEST than for manual calibration. This shows the relatively low efficiency of the model for low flows compared to high flows, though the overall model performance is rated good. It can be justified by the fact that lack of interest for low flows usually causes incorrect discharge data to be collected and/or calculated in Ethiopia, based on our experience of discharge data from the Ministry of Water Resources. This would contribute for low flows to be less efficiently calibrated and simulated relative to high flows where better quality data are usually collected.

Table 3 Statistical model performance indicators.

Model Performance Indicators	Manual Calibration	PEST Calibration	Validation
C1: Model bias for evaluating the ability of reproducing Water Balance	0.63 (4.66%)	-0.34 (-2.54%)	0.54 (12.15%)
C3: Model efficiency (Nash-Sutcliffe coefficient) for evaluating the ability of reproducing Stream Flows (NS)	0.69	0.70	0.85
C4: Model efficiency (Nash-Sutcliffe coefficient) for evaluating the ability of reproducing Low Flows (NSL)	0.88	0.75	0.83
C5: Model efficiency (Nash-Sutcliffe coefficient) for evaluating the ability of reproducing High Flows (NSH)	0.83	0.83	0.93

Fig.8 shows the graphical comparison between the observed and the calculated daily stream flow hydrographs during the calibration period (01 January, 2000 to 26 December, 2001). As it is shown from the graph, the simulated daily stream flow is generally in good agreement with the observed daily flows (daily stream discharges expressed in m3/s where 1 m3/s = 86,400

m3/day) except for some deviations of measured outliers. This is further proven by model performance indicators as shown in Table 3 with model efficiency for evaluating the ability of reproducing total stream flows (NS) value of 69.8%, model efficiency for evaluating the ability of reproducing low flows (NSL) =74.8% and model efficiency for evaluating the ability of reproducing high flows (NSH) =83.3%. The model is able to reproduce the observed water balance with 2.54% under estimation (Bias=-2.54%).The model performance indicators (NSL and NSH) illustrate that the model performs better for high flows than for low flows by about 8.5% model efficiency difference.

As observed in the hydrographs below, the high flows occur during summer season (usually become high at the middle of August and erratically decrease to very small values at the end of September. This goes in line with the rainfall but with a time lag. However, this lag in time is small compared with the big areal extent of the basin. This can be due to the fact that most of the discharge at the basin outlet is from surface runoff (from water balance calculation) and as shown in Fig.7, it takes comparatively short time (only about 6.6 days on average) to reach the outlet. The lag time, shown in Fig.8 for calibration and Fig. 9 for validation, is the reflection of this fact.

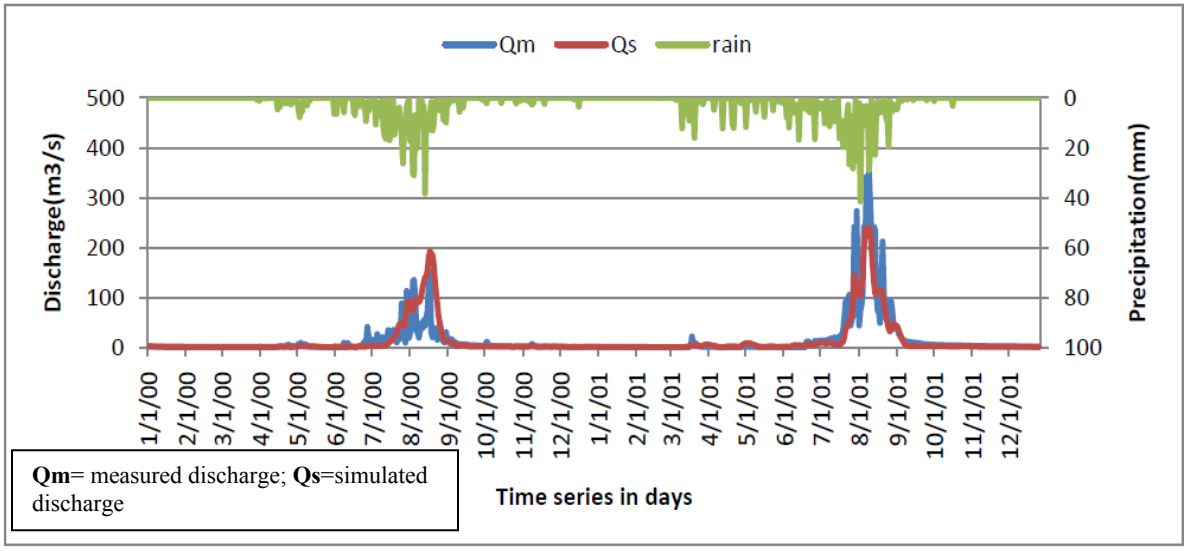

Fig. 8. Graph of simulated stream flow versus measured discharge with rainfall at the Geba basin outlet for the calibration time period (January 01, 2000 to December 26, 2001)

The model validation was done for the time period from December 27, 2001 to December 18, 2003. Fig. 9 shows graphically the simulated and measured discharges at the basin outlet and their correspondence with rainfall amount. The simulated hydrographs of both the low and high flows have a good match with the observations. However, some overestimation (like from July 26, 2003 to August 11, 2003) and under estimations like in the month of January, 2002 and starting from October 02, 2003 to December 18, 2003 are observed. Generally, the WetSpa model has still good simulation performance as shown in Table 2 for the validation, whereby NS for evaluating the ability of reproducing whole stream flows is 85.1%. 92.5% and 82.9% are NS values for high and low flows respectively. The model bias value is 12.15% which is comparatively high.

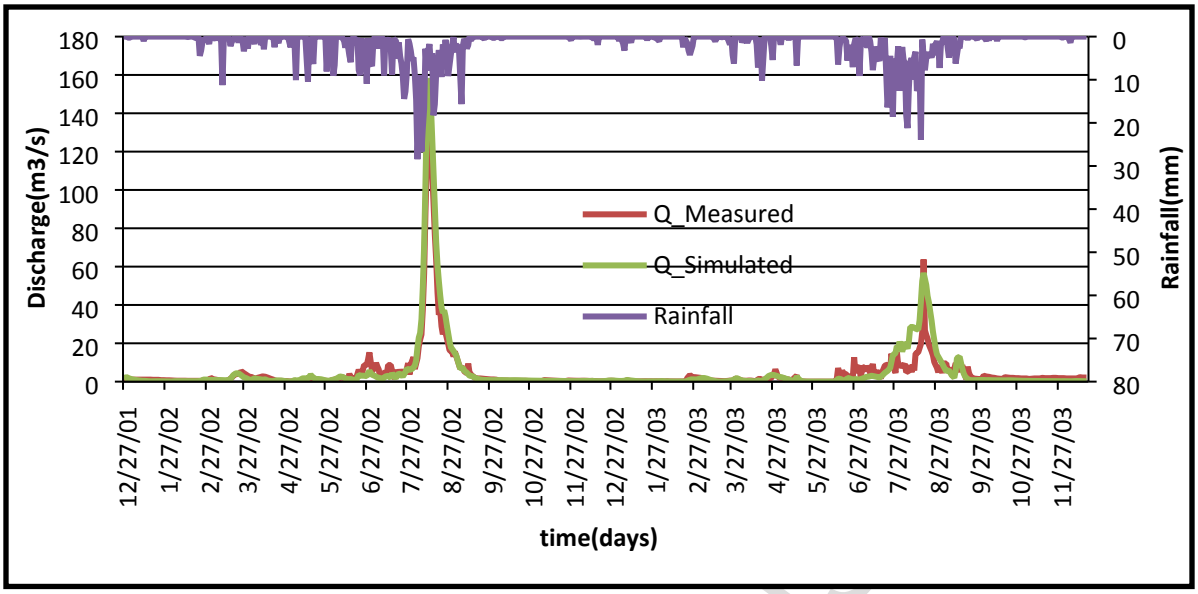

Fig.9. Graph of simulated stream flow versus measured discharge and rainfall at the Geba basin outlet for the validation time period (December 27, 2001 to December 18, 2003).

3.3. Water Balance

Table 4 shows the water balance for the Geba basin over the whole simulation period. Due to the relatively low forest (tree) coverage, as depicted from the land-use map of the basin, only about 3.8% of the total precipitation was intercepted by the plant canopy. 87.5% infiltrated into the soil, and 7.2% was lost as surface runoff. 94% lost as evapotranspiration to the atmosphere, 11.4% percolated and recharged the groundwater reservoir, and 10% became runoff (total river discharge at the outlet or sum of surface runoff, interflow and groundwater flow). The percentage sum of these three components was more than 100% or the actual evapotranspiration (94 %) was more than the infiltrated water (87.5%) to the subsurface in the simulation period. This shows that some amount of the water lost through evapotranspiration was from the accumulated deep groundwater source of the previous years though the major part was from the precipitation of the simulation period. 72.6% of the total runoff (river discharge) is contributed by surface runoff (overland flow), 24.1% and 3.3% was from interflow (unsaturated zone or

lateral flow) and groundwater flow respectively. This shows the relatively small contribution of groundwater to the river discharge compared to the groundwater recharge. However, when we look at the groundwater balance, there is groundwater level reduction by 9.1 mm (0.34% storage lost) during the simulation period although the groundwater discharge to the river is insignificant. This supports the idea that measurable evapotranspiration is taking place from the groundwater of the basin, although most evapotranspiration is from the unsaturated soil zone before percolation and recharging of the groundwater.

Table 4 Water balance estimation at Geba basin for the whole simulation period (from January 1, 2000 to December 18, 2003).

Water Balance Component	Total Measured value(mm)	Total Calculated value(mm)	Percentage (%)	Mean value (mm/day)	Maximum value(mm/day)
Precipitation	2,689.6	2,688.5		1.858	41.48
Interception		101.1	3.76	0.070	0.65
Infiltration		2,352.6	87.51	1.626	29.51
Soil Moisture difference		-92.4	-3.44	164.869	269.64
Evapotranspiration	6,474.1 (potential)	2,528.1 (actual)	94.03	1.747	7.06
Percolation (groundwater recharge)		307.7	11.44	0.213	8.53
Surface Runoff		194.1	7.22	0.134	18.60
Interflow		64.4	2.40	0.045	4.70
Groundwater Flow		8.9	0.33	0.006	0.04
Runoff	265.4	267.4	9.95	0.185	20.77
Groundwater Storage difference		-9.1	-0.34	16.629	113.25

Out of the 2,353 mm infiltrated water from 01 January, 2000 to 18 December, 2003, 13% percolates down the root zone and recharges groundwater, 2.7% becomes lateral flow and the largest part (about 84.2%) went from the root zone to the atmosphere as evapotranspiration. This is directly related to the dominant land-use types of the area. As it can be shown from the land-use percentage graph (Fig.3), about 87% of the total catchment area, was covered by land-use classes with shallow rooted vegetation (mixed forest, closed and open shrub, grassland and crop) type. Only about 3.3% of the vegetation was forest, where trees could probably reach the groundwater and transpire water from depth. The transpiration from groundwater storage can be

calculated from the percolation amount from which the difference in groundwater storage is subtracted. It is 317 mm in total, comprising only 12.5% of the total evapotranspiration while about 83.5% (2110 mm) of the total evapotranspirated water was from the root zone, and the rest which was about 4% (101 mm) of the total evapotranspiration was from direct evaporation of the intercepted water. The groundwater depth in Geba catchment is generally deep; there are places with depth of about 200 m though there are some places with shallow groundwater depth such as hand dug wells or shallow drilled wells (Tesfagiorgis et al., 2011). This is the reason for the low amount of evapotranspiration from the saturated zone.

The model shows that a high percentage of infiltrated water was lost by evapotranspiration, which could be mainly attributed to the climatic conditions and partly to the land-use of the area as described above. The high temperature and wind speed, the long sunshine hours and the low relative humidity intensify this phenomenon. As can be observed from Table 4, there is a high difference between actual and potential total evapotranspiration values. This can be justified through the fact that the region in which the basin is located is arid and hence the annual potential evapotranspiration significantly exceeds annual precipitation and thus actual evapotranspiration. This is reflected in the simulated balance shown in Table 4.

3.4. Groundwater Recharge

Recharge to the groundwater aquifer system in the study area is mainly through the infiltration of rainfall and some through seepage from surface water bodies such as micro to medium scale dams and streams. Precipitation induced recharge generally occurs throughout the study area with the exception of groundwater discharge zones (near major streams and ponds) and area covered by impervious surfaces like urban and bedrock, which is rather small in areal coverage (Fig. 3).

3.4.1. Temporal variation of groundwater recharge

As shown in the Fig. 10 and 11, monthly and average monthly groundwater recharges follow the trend of both rainfall and infiltration. Recharge is high during the rainy summer season and zero during the dry winter. The figures also show the relatively high (compared with the small rainfall amount) infiltration rate during spring (months having small amount of rainfall such as February, March, April and May) in contrast with the summer months (June, July and August). This can be justified by the low antecedent moisture content of the soil as it is preceded by a long dry period. Most of the water goes in moistening the soil rather than leaving as surface runoff. In addition, the desiccation cracks in the dry period on the clay and clay loam soil types (measured up to half a cm depth), observed during field visits, also play major role in enhancing the initial infiltration which later (in the course of rainy season) would be closed with the full moistening and hydration of the clay minerals. This definitely contributes in reducing actual runoff. Similar results were obtained by Zenebe et al. (2013) during their surface runoff calculation, based on automatic daily discharge data collected (for four years) on the major sub-catchments of the basin. The percolation or recharge during spring season is nearly zero. Because free water for recharge from the soil zone is possible after the field capacity of the soil is completely filled. Both groundwater recharge and interflow are following the same trend and become maximal during the rainiest month of August and decline immediately after rainfall ceases around the end of September. The mean annual recharge value varies from about 45 mm in the year 2003 to 208 mm in 2001.This is due to the rainfall amount difference of these years which is 516 mm and 1454 mm, respectively.

The average annual recharge for the whole study area is about 99 mm per year which is 11.4% of the total annual rainfall. Gebreyohannes et al. (2013) using the WetSpass model

estimated recharge as 6% of the rainfall, which is about half of the new result. This could be due to the following reasons. The first reason is the time scale used in the two studies: daily and long term seasonal time-scales respectively. Shorter time-scales are known to result in larger values of groundwater recharge (Walraevens et al., 2009). The second reason is that in this study, the lower part of the basin is excluded (which was found to be very low recharge area in recharge classification of Gebreyohannes et al. (2013), while the high recharging central and Northern part are included in this study. The third and most important reason is the conservation practices applied in the area, after the study by Gebreyohannes et al. (2013), which changed the land-use type to more recharge favorable types i.e. from the bare soil land, with high runoff coefficient and low infiltration capacity, to shrub land (table 1) having relatively high infiltration potential, as shown in model default values in Liu and De Smedt (2004). This is also supported by the higher runoff (18%) and lower evapotranspiration (76%) found in Gebreyohannes et al. (2013), while they are 7.2% and 94% (higher than infiltration) respectively in our work. These all together increased the average result shown in this study.

The water balance calculation (modeling) being based on finer time scales (daily in this case) which is close to each rainfall event, the primary source of water in the balance variables, is more realistic and reasonable than the estimations made on long term averages by Gebreyohannes et al. (2013). Layer by layer water balance calculation, taking the daily records of the meteorological variables (used in rainfall and PET) and river discharge measurements, close to the event (reality), enabled to estimate surface runoff, actual ET, inter flow, interception, soil moisture, and depression storage in a better way than using seasonal average data. As a result, the simulated recharge is more realistic. The runoff model developed for Agulae catchment by Fenta et al. (2017) and ran for the period 2000-2012 revealed streamflows

decrement during wet season and increment during dry season by 49% and 57%, respectively, with no significant annual and temporal rainfall variations. It shows the increasing trend on infiltration, and then groundwater recharge, attributed to the land-use change of the study area, which is in line with our study.

The rainfall in the study area didn't show any trend for the simulation period but recorded highest for 2001, preceded and followed by relatively low rainfall years, which is in agreement with Hadgu et al. (2013) who noted that rainfall is highly variable with no meaning full trend for seasonal and annual totals. As a result, the percolating water doesn't follow either increasing or decreasing trend with time. The mean monthly recharge value is high for August with value of 73 mm, July is the next having 19 mm; and September and June follow with 2.3 mm and 1.3 mm, respectively. The lowest recharge month is December (0.08 mm).

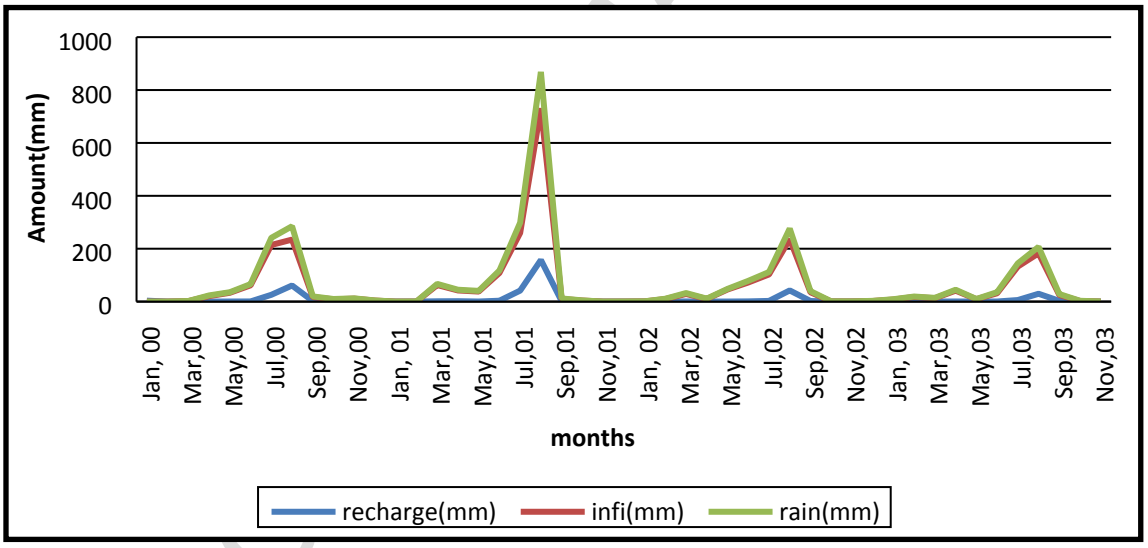

Fig. 10. Monthly recharge, infiltration and rainfall over the whole simulation period

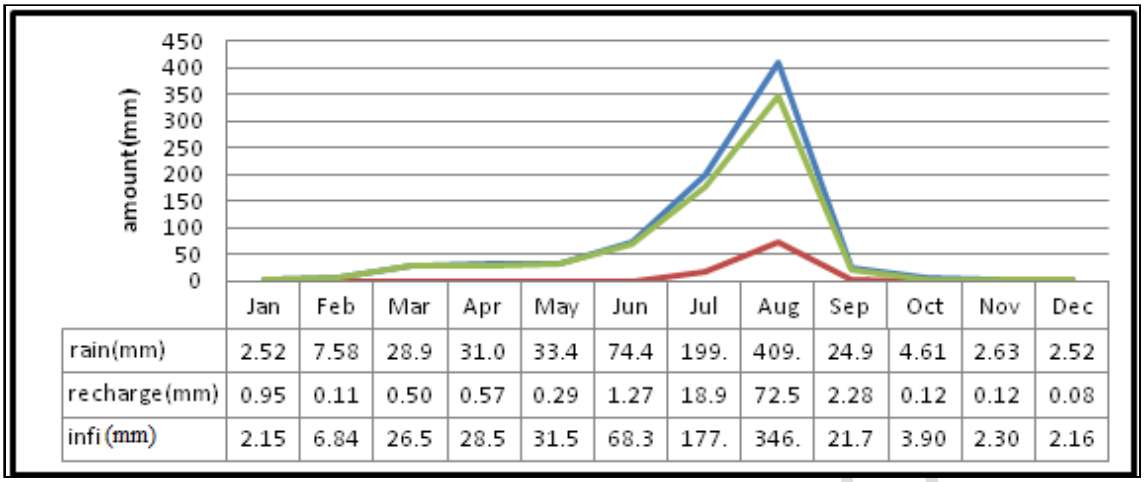

	Jan	Feb	Mar	Apr	May	Jun	Jul	Aug	Sep	Oct	Nov	Dec
rain(mm)	2.52	7.58	28.9	31.0	33.4	74.4	199.	409.	24.9	4.61	2.63	2.52
recharge(mm)	0.95	0.11	0.50	0.57	0.29	1.27	18.9	72.5	2.28	0.12	0.12	0.08
infi (mm)	2.15	6.84	26.5	28.5	31.5	68.3	177.	346.	21.7	3.90	2.30	2.16

Fig. 1. Mean monthly recharge, infiltration and rainfall over the whole simulation period

3.4.2. *Spatial Distribution of Recharge*

WetSpa allows spatial variation of its parameters over a particular catchment by combining information from the three basic maps of land-use, soil and topography, which results in a more accurate representation of natural hydrological processes (Liu and De Smedt, 2004). Moreover, variation in the hydro(meteoro)logical variables (PET and precipitation) gives a highly spatially varied recharge of Geba basin.

The average annual percolation or simulated groundwater recharge spatially ranges from zero to 371 mm. It is reclassified into six recharge classes as shown in Fig. 12. Areas which are labeled as water body land-use class have a value of around 0 mm or 1.0 mm, regardless of other recharge conducive conditions (such as flat topography, porous and permeable soil type, high rainfall, etc.). This is because they are considered as zones of discharge or impervious percentage is 100% (Liu and De Smedt, 2004). As expected, areas with a soil having a good hydraulic conductivity such as sand, sandy clay and sandy loam have high recharge value if the rainfall is either not significantly low or/and the land-use is no water body or urban. The sandy soil in the Northern parts of the catchment is anticipated to have a very high recharge amount, except those

parts covered by water body. However, the relatively lower rainfall amount recorded, to high extent, and the steep topography (Fig. 7), to some extent cause part of the area to have medium and low recharge classes. In some cases, the recharge classes follow the soil types, where hydrologically very different soil groups are close to each other (Fig. 4).

There is a sharp contact between recharge classes (with straight lines class boundaries) which is deviated from the reality to a certain extent (especially around class contacts). This cannot be attributed to any of the other groundwater recharge influencing factors, but is due to the rainfall interpolation effect of the Thiessen polygon method. If we compare with the Thiessen polygon map (Fig.6), we can recognize these lines. Indeed, this is due to interpolation of rainfall from few meteorological stations for such big area, and strong rainfall variability (Hadgu et al., 2013; Nyssen et al., 2005). According to Nyssen et al. (2005), topographical factors, especially general orientation of the valley and slope gradient over longer distances, determine the spatial distribution of rainfall. The model quality of WetSpa, largely depends on quality of the meteorological data (Porretta-Brandyk et al., 2010). Abrupt changes from one Thiessen polygon to the other are observed in the spatial maps. This can be improved if many gauging stations are installed and included in the interpolation. This is the main limitation in the study. The influence of other climatic variables such as minimum and maximum temperature, wind speed, sunshine hours, and relative humidity would play some role through their effect on the PET, the spatial variation of which remains limited.

Groundwater recharge and other hydrologic components were found to be highly controlled by geology. The expected high potential surface runoff and low infiltration rate, estimated from the characteristics of soil types, slope, and land-use are not attained in this model.

The rainfall character, lithology type and geological structures (Fig. 2) are rather mainly the dictating factors for the share of the balance components.

Geology is one of the controlling factors for soil, topography, and land-use. The three regional normal dip-slip faults in Fig. 2 (Mekelle, Chelekot, and Wukro), for example, are the reasons for the existence of the elevated and sloping topography, and exposure of deeper stratigraphical sequences (Precambrian and deeper Mesozoic sedimentary), where the fault planes are sloping and the blocks (walls) are relatively flat. In addition, the presence of the plunging, Negash Synclinal fold (Fig. 2), is the primary factor for the rugged topography in the metamorphic terrain of the basin. Besides, the local faults and folds have also paramount importance in the evolution of the geomorphology and the topography (slope), and thereby the surface runoff and the infiltration of each rainfall event.

Generally, soil is the weathering product of rock, further subjected to post processes, the magnitude of which depends on the soil type and its physical, biological, and chemical characteristics. For geological, geomorphological and hydrological reasons, most of the soil coverage in the basin is residual soil type rather than transported, with laterally uniform soil (in porosity, permeability, water holding capacity, e.t.c), as the soil originated from one lithology or genetically similar lithology types. As a result, unlike transported soil, common in the different river basins of Ethiopian highlands, the relative uniformity of the properties important for the hydrology within one soil class, better fits to the model assumption of homogeneity and isotropy (Liu and De Smedt, 2004). The texture of soil depends on the parent rock type, weathering magnitude and rate, weathering type (either mechanical or chemical or combination), biological mixtures, and other physico-chemical factors. When we consider soil types and underlying lithological formations, there is no unique relation i.e. a given soil type is multi-parental and

613 overlies different rock units (Fig. 2 and 4). This shows the high controlling power of other soil
614 formation factors rather than lithology. However, good correspondence is observed between
615 shale, marl, and limestone varieties, that are usually found in association both in the Antalo
616 Limestone and Agulae Shale Formations, with clay loam and clay soil types which are known to
617 be weathering products of these litho-units.

618 Furthermore, Enticho sand stone and volcanic rock varieties, in the northern most part of
619 the basin, are both covered by sandy soil where the field study showed different mineralogical
620 composition of the soil on the two rock types: olivine-pyroxene-plagioclase rich on the volcanic
621 rock and quartz rich on the sandstone. Likewise, the other soil types (Fig. 4) are formed from
622 different parent rocks having different minerals with different properties though grouped in one
623 class on the basis of texture. This variation causes hydrological processes to spatially vary in the
624 root zone (e.g. soil moisture content variation in different clay mineral varieties). However, this
625 difference only affects the initial moisture content of a given rainy season which has insignificant
626 importance in long term hydrological simulations like in this study (Liu and De Smedt, 2004).
627 Furthermore, the depth of the soil-rock interface which is an important factor for percolation,
628 depends on the geology; this was accordingly set up in the model. However, the model is not
629 flexible enough to illustrate the spatial variation within a soil class.

630 In general, geology affects the spatial distribution of the soil which is one of three
631 important spatial factors considered in the study. Similarly, the geology and geomorphology are
632 among the important factors upon which the land-use/landcover depends. More vegetated land is
633 found on volcanic and carbonate rocks than on shale (Figs. 2 and 3). This is due to the suitability
634 of the soil composition which is mostly reflecting the underlying rock.

In conclusion, the spatial distribution indirectly depends on geology of the basin. Direct consideration of both lithological and geological structure as an independent input is not made in this work though it is unwise to underestimate their effect in influencing groundwater recharge. However, their summative effect in affecting the overall basin-wise hydrologic budgets for each component (recharge, runoff, AET, soil moisture), is well accounted during model calibration and validation based on observations.

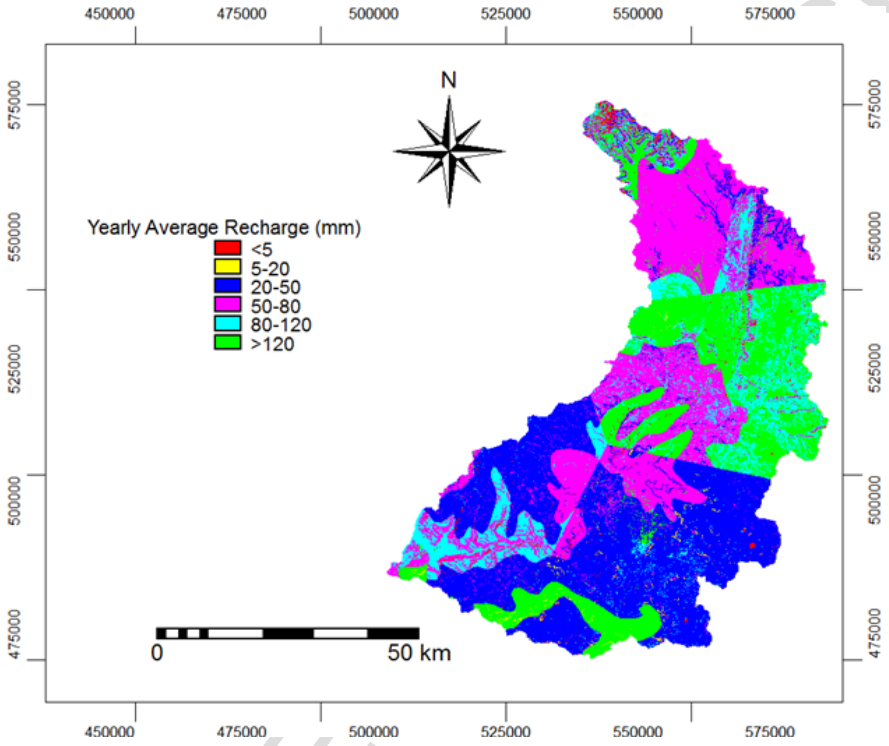

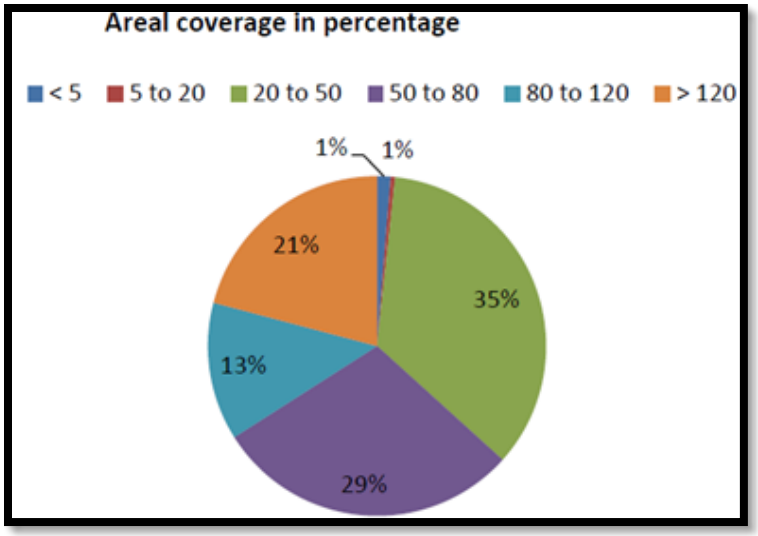

643

644 **Fig. 12. Spatial distribution map of mean annual recharge (a) and areal coverage of recharge classes in**

645 **percentage in the Geba catchment (b)**

646 Arefaine et al. (2012) applied the WetSpass model to simulate the hydrological

647 components of Illala catchment, located in the lower south central part of the Geba basin (Fig. 1),

648 by using the land-use prepared from satellite images in parallel with this study. According to

649 their calculation, the mean annual groundwater recharge, surface runoff, and actual

650 evapotranspiration (ET) are 12%, 7%, and 81% of the precipitation, respectively, which is closer

651 to our result.

652 Field et al. (2017) modeled the groundwater flow system in the well field of Aynalem

653 river (tributary of Geba) catchment, covering an areal extent of 102 km^2, located near to Mekelle

654 city (Fig.1) using MODFLOW. In their model, they used 9% (of mean precipitation) recharge

655 input, determined by water balance and base flow separation techniques. Most of this area laid in

656 class 3 (20-50 mm/year) recharge class (Fig.12) of our groundwater recharge classification. The

657 recharge to precipitation percentage, taking the average annual class to its corresponding mean

annual precipitation at the Mekelle-Quiha meteorological station, accounted to be 11% in this study, which is close to 9% found by (Field et al., 2017).

Tilahun and Merkel (2009) used WetSpass to see the spatial variation and the controlling physical and hydro-meteorological factors of groundwater recharge, surface runoff and ET, in a similar semi-arid environment called Dire Dawa basin, in eastern Ethiopia, having areal coverage of about 920 km^2. According to this work, 5%, 20% and 75% of rainfall were the average annual values for recharge, surface runoff and ET, respectively. Their lower value for recharge and higher for surface runoff, though the area is similar in climatic conditions, topography, and soil type with Geba basin, is mainly due to the higher impervious percentage of the land use i.e. the bare land in Geba is about 10% while it is 26% for Dire Dawa during the corresponding study times.

3.5. Spatial and temporal distribution of surface runoff, Soil moisture and Evapotranspiration

Generally, the variations both in time and space of surface runoff, soil moisture and ET, are directly related to rainfall amount and intensity, land-use, soil, and slope, geology (lithology and geological structures) and other climatic conditions like wind speed, moisture carrying capacity, atmospheric moisture content, temperature and length of sunshine hours.

Surface runoff depends on the rainfall characteristics (amount and intensity), soil type, slope, land cover, antecedent soil moisture, and depression characters of an area. The potential runoff, in this study is based solely on physiographic features of the area such as soil type, land-use, and slope maps using the default values, based on literature, for different possible combinations (Liu and De Smedt, 2004). The mean annual actual runoff simulated (7.2% of

680 precipitation) is very low, compared to the corresponding predicted potential runoff (shown in
681 the potential runoff coefficient map in Fig. 6). This illustrates that the mean and total amount of
682 actual runoff is highly controlled and responsive to other factors than the basins physiographic
683 features, though the spatial distribution is partially correlated with these factors.

684 According to Liu and De Smedt (2004), the proportion of runoff increases along with the
685 increase of rainfall intensity up to a stage at which potential runoff coefficient is achieved. In
686 WetSpa an empirical exponent, the surface runoff exponent for a near zero rainfall intensity
687 (K_run), is assumed to be a variable starting from a higher value for a near zero rainfall intensity,
688 and changing linearly to 1 along with the rainfall intensity. In this model, K_run is about 8.5
689 (table 2), which is relatively high and shows the low rainfall intensity of the area. Mainly low
690 daily rainfall amount is being recorded in the area, thereby producing low runoff, contrary to the
691 prediction in the potential runoff coefficient. A good correlation between simulation and
692 measurements is found for the high streamflows (much better than for the low flows) (C5 in table
693 3; Fig. 14). This shows the effectiveness of the developed model in simulating the runoff.
694 Similarly, Zenebe et al. (2013) observed that several smaller rainfall events recorded by rain
695 gauges, could not be detected in the runoff response and vice versa. This could be ascribed to the
696 local character of many rainstorms. In addition, their estimated runoff coefficient negatively
697 correlated with the areal fraction of limestone outcrops in the catchments, indicating runoff
698 transmission losses from their specific sub-catchment to sub-catchment runoff analysis. Besides
699 to the rainfall characteristics, the common karsts and sinkholes in the marl-limestone, shale-marl-
700 limestone, limestone-marl, meta-limestone rock units, and in limestone-dolomite-gypsum beds of
701 Agulae shale formation, covers the central part of the study area (Fig. 2), playing significant role

in controlling the hydrologic cycle and the share of the water balance components. They enhance infiltration, and significantly lessen runoff.

Moreover, the geological structures (major and minor faults, joints, sedimentary inter-beddings, and foliations), reduce surface runoff as the relatively high porosity, and hence permeability through the openings cause infiltration to the subsurface, rather than producing overland flow, even in high rain events. These geological features i.e. karsts on chemical sedimentary and meta-sedimentary rocks, and geological structures in all rock types, which both result in effect lowering surface runoff and increasing infiltration, are the major reasons for the low observed runoff contrary to the expectation. The very low correspondence between actual and potential runoff, was the primary causative factor for the unsuccessfulness of the different small and medium scale dams in the area (Berhane et al., 2017; Gebreyohannes et al., 2013; Taye et al., 2013; Zenebe et al., 2013), wherein the actually stored reservoir water quantities much lower than the designed. Their hydrological design was based, solely on surface physiographical catchment characteristics regardless of rainfall character, geology or stream discharge measurements.

The spatial distribution of potential surface runoff is shown in Fig. 13. It follows the distribution and interplay of rainfall amount, soil type, slope, and land-use. Generally sand, sandy clay and sandy clay loam soil classes have lower runoff, up to annual runoff amount of 50 mm, expected from the runoff coefficient map (Fig. 7), due to their high hydraulic conductivity value. A high value observed in the sandy class is due to the totally impervious land-use “water body”. The loam and sandy clay loam in the upper part of the catchment have got sharply separated runoff classes (Fig. 13). This is because of the rainfall interpolation effect (Thiessen polygon). In the lower (southeastern), the middle and uppermost (northern) part of the

catchment, bare land and urban classes are found to have relatively higher runoff. Generally, the primary factors for the spatial distribution of actual surface runoff are rainfall amount and partly soil and land-use in the study area. The highest runoff class in the middle of the study basin (Fig. 13) is attributed to the Thiessen polygon of relatively highest rainfall registered at Wukro meteorological station (Fig. 6) despite soil types are impervious: clay and clay loam (Fig. 4) .

Fig. 14 shows the spatial distribution of annual actual evapotranspiration in the Geba catchment. It shows that the evapotranspiration class distribution is highly dependent on rainfall. Since our study area belongs to an arid region, the most important determining factor for evapotranspiration is water availability followed by the land-use and soil characteristics. The spatial variation of the climatic conditions (temperature, humidity, sunshine hours, and wind speed), on which evapotranspiration depends, are not significant in the study basin. This can be inferred by relating the actual evapotranspiration map (Fig. 14) with the elevation map (Fig. 1), which is an important factor for local climatic variation of an area. The influence of soil conditions is observed visibly in the upper part between sand and clay loam. Land-use plays similar role as soil, with high values for vegetation coverage.

The temporal variations of evapotranspiration, soil moisture and surface runoff with rainfall are shown in Fig. 15. They strictly follow the trend of rainfall, which is the primary source of water for all these hydrological processes. However, around the beginning of January, 2000, the soil moisture content is high, which also made the evapotranspiration relatively significant. This might be due to rainfall that occurred during autumn season (before January) in 1999 where sometimes happens in the region. The effect of groundwater is minimal as the water table depth is high. Evapotranspiration, and to some extent soil moisture respond with some lag in time, as it takes time to infiltrate into the soil especially for those soils with high field capacity

like clay. The residual soil moisture content is high, due to the dominant soil coverage of the area by clay, clay loam and loam soil types.

Though the peak rainfall amount varies in the four rainy seasons of the simulation period, the actual evapotranspiration does not show variation (is almost equal). This leads to a conclusion that during the rainiest month of August, the actual evapotranspiration is almost equal to the PET value and the influencing factors are weather variables (other than rainfall), vegetation and soil conditions rather than the water availability. Moreover, a high surface runoff occurred on August 2, 2001, amounting to 18.6 mm. When it is compared with other peak runoff periods, it is significantly increased with relatively small increment in rainfall. For example, a maximum of 38.3 mm rainfall was recorded on August 13, 2000, from which only 8.2 mm left as surface runoff, while 18.6 mm surface runoff had happened with 41.5 mm rain amount (on August 2, 2001). This high increment in surface runoff while the precipitation didn't rise significantly can be ascribed to the intensity of the rain and the high moisture condition of the soil (which restricts the infiltration). The spatial distribution of the soil moisture is mostly depending on soil type rather than land-use and rainfall.

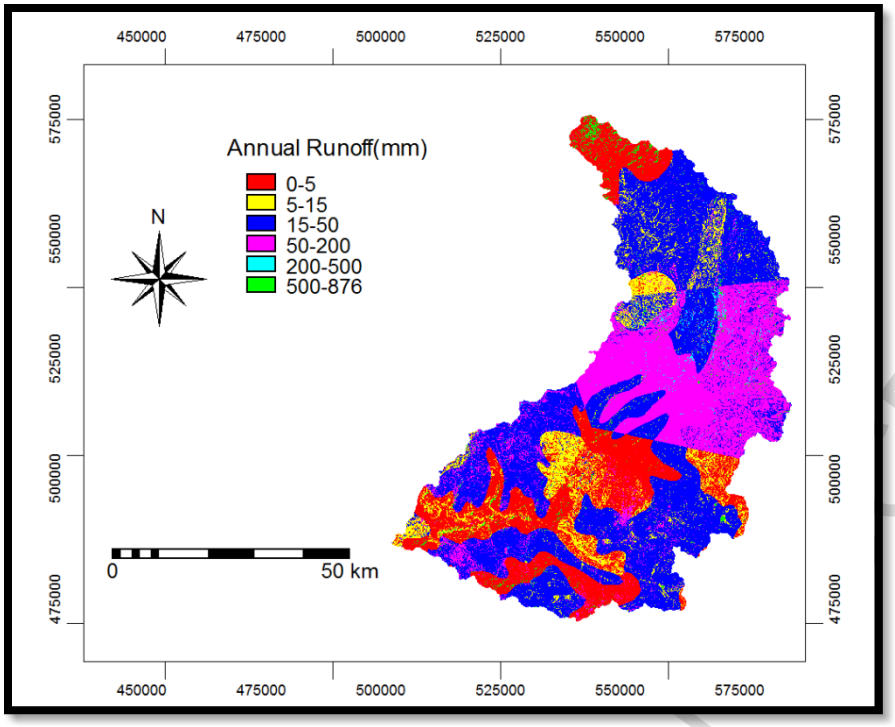

763

764 **Fig. 2. Annual actual surface runoff map of Geba basin**

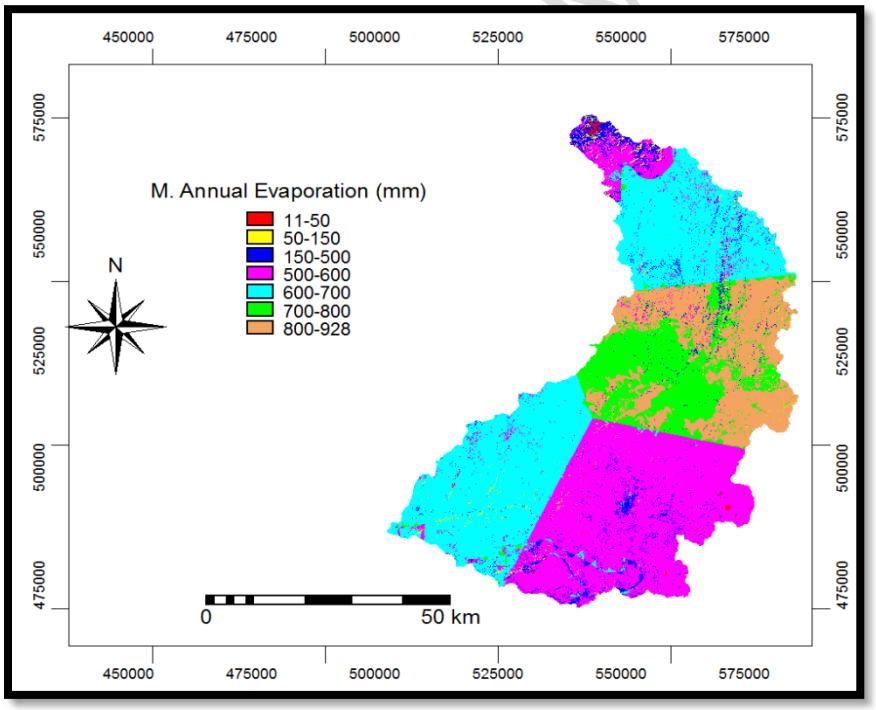

765

766 **Fig. 3. The mean annual evapotranspiration of Geba basin**

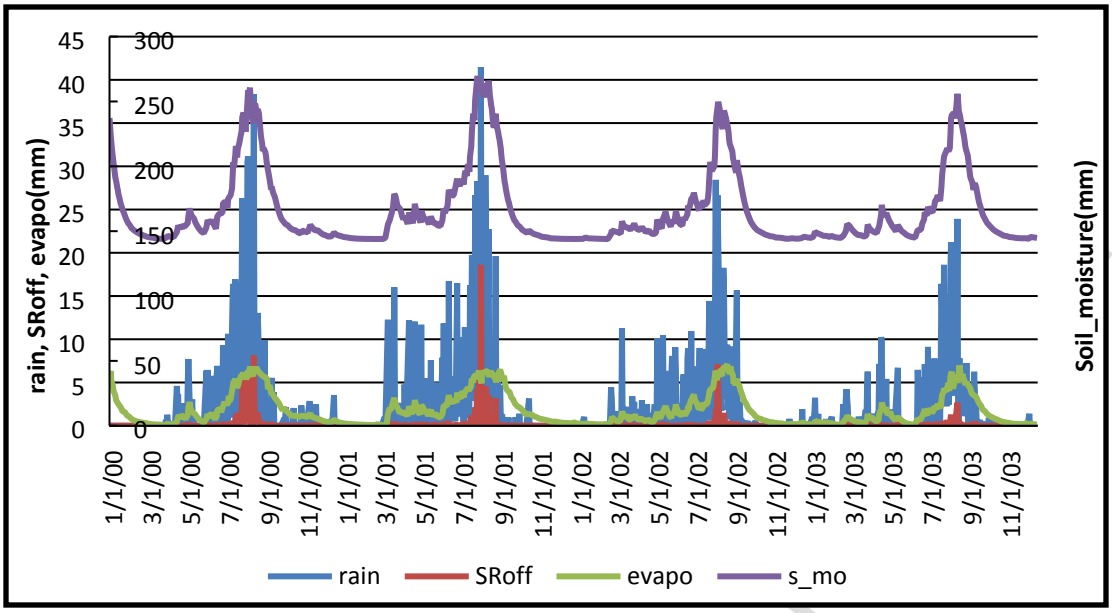

Fig. 4. Daily evapotranspiration, surface runoff and soil moisture with rainfall over the whole simulation period

4. Conclusion

A GIS based, physically distributed watershed model called WetSpa was applied to Geba catchment, covering an area of 4,249 km^2 in Northern Ethiopia. The model was effectively applied to determine the spatial and temporal variation of groundwater recharge, in the period of January 01, 2000 to December 18, 2003. This spatially distributed hydrologic model was simulated using daily time scale in this particular study. The spatial properties of input meteorological parameters (rainfall and PET), were interpolated using Thiessen polygons, where the altitude variation effect of the gauging stations corrected by linear topographic correction method. The model uses a 90 m by 90 m resolution DEM, land-use and soil type map for taking spatial information into account and derives all required hydrologic model parameters in spatially distributed manner within a GIS framework.

The model was both calibrated and validated by about two years of meteorological and discharge data. The model performance indicated by values obtained by calibration both

783 manually and by PEST, is generally fair. It has a bias of -2.54%, NS=69.83%, NSL=74.78% and
784 NSH of 83.26%. The simulated and measured daily stream hydrographs are generally in good
785 agreement as well when visually observed.

786 There is high variation of recharge both spatially and temporally. The spatial rainfall
787 variation and characteristics, followed by the soil type and land-use, and to certain extent the
788 slope control the spatial distribution. The geology also plays an important role. For the temporal
789 variation of recharge, rainfall is the determinant factor, and to some extent also the soil type,
790 through the antecedent soil moisture variation, during the summer and spring or start of rains
791 for a year. The other climate variables have played role in determination of the total or mean
792 values, but are insignificant for the time variation of recharge.

793 *Acknowledgement*

794 The Belgian Development Cooperation (VLIR-UOS) sponsored this work. Thus the
795 authors acknowledge VLIR-UOS for the funding of the research project. We are grateful to the
796 National Meteorological Service Agency of Ethiopia (Mekelle Branch) for making
797 meteorological data available. We would like to pass our great appreciation to Dr. Hadush
798 Goitom for his technical support during the model development of the study area. The first
799 author would also acknowledge Ghent University and Free University of Brussels for their
800 support during his study stay at the time of this research work.

801 *References*

802 Adem, G., Batelaan, O., 2006. Modeling groundwater-surface water interaction by coupling MODFLOW
803 with WetSpa, in: Geophysical Research Abstracts. p. 3181.

804 Alemayehu, F., Taha, N., Nyssen, J., Girma, A., Zenebe, A., Behailu, M., Deckers, S., Poesen, J., 2009. The
805 impacts of watershed management on land use and land cover dynamics in Eastern Tigray

(Ethiopia). Resour. Conserv. Recycl. 53, 192–198. doi:10.1016/j.resconrec.2008.11.007

Allen, R.G., Pereira, L.S., Raes, D., Smith, M., 1998. Crop evapotranspiration-Guidelines for computing crop water requirements-FAO Irrigation and drainage paper 56. FAO, Rome 300, D05109.

Arefaine, T., Nedaw, D., Gebreyohannes, T., 2012. Groundwater Recharge , Evapotranspiration and Surface Runoff Estimation Using WetSpass Modeling Method in Illala Catchment , Northern Ethiopia 4, 96–110.

Batelaan, O., De Smedt, F., 2001. WetSpass: a flexible, GIS based, distributed recharge methodology for regional groundwater modelling. IAHS Publ. 11–18.

Berhane, G., Amare, M., Gebreyohannes, T., Walraevens, K., 2017. Geological and geophysical investigation of water leakage from two micro-dam reservoirs: Implications for future site selection, northern Ethiopia. J. African Earth Sci. 129, 82–93.

Bouraoui, F., Vachaud, G., Li, L.Z.X., Le Treut, H., Chen, T., 1999. Evaluation of the impact of climate changes on water storage and groundwater recharge at the watershed scale. Clim. Dyn. 15, 153–161.

Brown, V.A., McDonnell, J.J., Burns, D.A., Kendall, C., 1999. The role of event water, a rapid shallow flow component, and catchment size in summer stormflow. J. Hydrol. 217, 171–190.

Carter, R.C., Parker, A., 2009. Climate change, population trends and groundwater in Africa. Hydrol. Sci. J. 54, 676–689.

Chormański, J., Batelaan, O., 2011. Application of the WetSpa distributed hydrological model for catchment with signi fi cant contribution of organic soil . Upper Biebrza case study. Ann. Warsaw Univ. Life Sci. - SGGW 43, 25–35. doi:10.2478/v10060-008-0090-6

Dams, J., Salvadore, E., Van Daele, T., Ntegeka, V., Willems, P., Batelaan, O., 2012. Spatio-temporal impact of climate change on the groundwater system. Hydrol. Earth Syst. Sci. 16, 1517.

De Vries, J.J., Simmers, I., 2002. Groundwater recharge: an overview of processes and challenges. Hydrogeol. J. 10, 5–17.

Doherty, J., 2010. PEST: Model independent parameter estimation, Watermark Numer. Comput. Brisbane, Queensland, Aust.

Eyasu, Y.H., 2005. Development and management of irrigated lands in Tigray, Ethiopia. Balkema.

Fenta, A., Yasuda, H., Shimizu, K., Haregeweyn, N., 2017. Response of streamflow to climate variability and changes in human activities in the semiarid highlands of northern Ethiopia. Reg. Environ. Chang. doi:10.1007/s10113-017-1103-y

Field, A.W., Kerebih, M.S., Keshari, A.K., Ph, D., Asce, M., 2017. GIS-Coupled Numerical Modeling for Sustainable Groundwater Development : Case Study of 22, 1–13. doi:10.1061/(ASCE)HE.1943-5584.0001444.

Freeze, R.A., 1969. The Mechanism of Natural Ground-Water Recharge and Discharge: 1. One-dimensional, Vertical, Unsteady, Unsaturated Flow above a Recharging or Discharging Ground-Water Flow System. Water Resour. Res. 5, 153–171.

Gebremeskel, S., Liu, Y.B., De Smedt, F., Hoffmann, L., Pfister, L., 2005. Assessing the hydrological effects of Landuse changes using distributed hydrological modelling and GIS. Int. J. river basin Manag. 3, 261–271.

Gebremeskel, S., Liu, Y.B., De Smedt, F., Hoffmann, L., Pfister, L., 2004. Analysing the effect of climate changes on streamflow using statistically downscaled GCM scenarios. Int. J. River Basin Manag. 2, 271–280.

Gebreyohannes, T., De Smedt, F., Walraevens, K., Gebresilassie, S., Hussien, A., Hagos, M., Amare, K., Deckers, J., Gebrehiwot, K., 2013. Application of a spatially distributed water balance model for assessing surface water and groundwater resources in the Geba basin, Tigray, Ethiopia. J. Hydrol. 499, 110–123.

Gebreyohannes, T., Smedt, F. De, Hagos, M., 2010. Tigray Livelihood Paper No . 9 Large-Scale Geological mapping of the Geba basin , northern Ethiopia.

Gebreyohannes, T., Smedt, F. De, Walraevens, K., Gebresilassie, S., Hussien, A., Hagos, M., Amare, K., 2017. Regional groundwater flow modeling of the Geba basin , northern Ethiopia. doi:10.1007/s10040-016-1522-8

Hadgu, G., Tesfaye, K., Mamo, G., Kassa, B., 2013. Trend and variability of rainfall in Tigray , Northern Ethiopia : Analysis of meteorological data and farmers ' perception. Acad. J. Agric. Res. 1, 88–100. doi:10.15413/ajar.2013.0117

Healy, R.W., Cook, P.G., 2002. Using groundwater levels to estimate recharge. Hydrogeol. J. 10, 91–109.

Imani, R., Ghasemieh, H., Ouri, A.E., 2016. Application and Calibration of WetSpa Hydrological Model for Daily Runoff Simulation for 2007-2008 to 2011-2012 Water years : A Case Study: Balokhluchay Watershed, Ardabil, Northwestern Iran. Int. Bull. Water Resour. Dev. 3, 140–152.

Karamage, F., Zhang, C., Fang, X., Liu, T., Ndayisaba, F., Nahayo, L., Kayiranga, A., Nsengiyumva, J., 2017. Modeling Rainfall-Runoff Response to Land Use and Land Cover Change in Rwanda (1990–2016). Water 9, 147. doi:10.3390/w9020147

Kassie, B.T., Asseng, S., Rotter, R.P., Hengsdijk, H., Ruane, A.C., Van Ittersum, M.K., 2015. Exploring climate change impacts and adaptation options for maize production in the Central Rift Valley of Ethiopia using different climate change scenarios and crop models. Clim. Change 129, 145–158.

Liu, Y.B., Batelaan, O., Smedt, F. De, Huong, N.T., Tam, V.T., 2005. Test of a distributed modelling approach to predict flood flows in the karst Suoimuoi catchment in Vietnam. Environ. Geol. 48, 931–940.

Liu, Y.B., De Smedt, F., 2004. WetSpa extension, a GIS-based hydrologic model for flood prediction and watershed management. Vrije Univ. Brussel, Belgium 1, e108.

876 Liu, Y.B., De Smedt, F., Pfister, L., Wu, B.S., 2002. Flood prediction with the WetSpa model on catchment
877 scale. Flood Def. '2002 499–507.

878 Nedaw, D., Walraevens, K., 2009. The positive effect of micro-dams for groundwater enhancement: a
879 case study around Tsinkanet and Rubafeleg area, Tigray, northern Ethiopia. Momona Ethiop. J. Sci.
880 1.

881 Nyssen, J., Vandenreyken, H., Poesen, J., Moeyersons, J., Deckers, J., Haile, M., Salles, C., Govers, G.,
882 2005. Rainfall erosivity and variability in the Northern Ethiopian Highlands. J. Hydrol. 311, 172–187.

883 Porretta-Brandyk, L., Chormański, J., Ignar, S., Okruszko, T., Brandyk, A., Szymczak, T., Krężałek, K., 2010.
884 Evaluation and verification of the WetSpa model based on selected rural catchments in Poland. J.
885 Water L. Dev. 14, 115–133. doi:10.2478/v10025-011-0010-8

886 Rwetabula, J., De Smedt, F., Rebhun, M., 2007. Prediction of runoff and discharge in the Simiyu River
887 (tributary of Lake Victoria, Tanzania) using the WetSpa model. Hydrol. Earth Syst. Sci. Discuss. 4,
888 881–908.

889 Safari, A., De Smedt, F., 2014. Improving WetSpa model to predict streamflows for gaged and ungaged
890 catchments. J. Hydroinformatics 16, 758–771.

891 Safari, A., De Smedt, F., 2008. Streamflow simulation using radar-based precipitation applied to the
892 Illinois River basin in Oklahoma, USA, in: Third International Scientific Conference BALWOIS.

893 Safari, A., De Smedt, F., Moreda, F., 2012. WetSpa model application in the Distributed Model
894 Intercomparison Project (DMIP2). J. Hydrol. 418–419, 78–89. doi:10.1016/j.jhydrol.2009.04.001

895 Scanlon, B.R., Healy, R.W., Cook, P.G., 2002. Choosing appropriate techniques for quantifying
896 groundwater recharge. Hydrogeol. J. 10, 18–39.

897 Seleshi, Y., Zanke, U., 2004. Recent changes in rainfall and rainy days in Ethiopia. Int. J. Climatol. 24, 973–
898 983.

899 Singh, V.P., Woolhiser, D.A., 2002. Mathematical modeling of watershed hydrology. J. Hydrol. Eng. 7,
900 270–292.

901 Smith, M., 1992. CROPWAT: A computer program for irrigation planning and management. Food &
902 Agriculture Org.

903 Tarboton, D.G., Bras, R.L., Rodriguez-Iturbe, I., 1991. On the extraction of channel networks from digital
904 elevation data. Hydrol. Process. 5, 81–100.

905 Taye, G., Poesen, J., Wesemael, B. Van, Vanmaercke, M., Teka, D., Deckers, J., Goosse, T., Maetens, W.,
906 Nyssen, J., Hallet, V., Haregeweyn, N., 2013. Effects of land use, slope gradient, and soil and water
907 conservation structures on runoff and soil loss in semi-arid Northern Ethiopia. Phys. Geogr. 34,
908 236–259. doi:10.1080/02723646.2013.832098

909 Taylor, R.G., Koussis, A.D., Tindimugaya, C., 2009. Groundwater and climate in Africa—a review. Hydrol.
910 Sci. J. 54, 655–664.

911 Tesfagiorgis, K., Gebreyohannes, T., De Smedt, F., Moeyersons, J., Hagos, M., Nyssen, J., Deckers, J.,
912 2011. Evaluation of groundwater resources in the Geba basin, Ethiopia. Bull. Eng. Geol. Environ. 70,
913 461–466.

914 Tilahun, K., Merkel, B.J., 2009. Estimation of groundwater recharge using a GIS-based distributed water
915 balance model in Dire Dawa , Ethiopia 1443–1457. doi:10.1007/s10040-009-0455-x

916 Walraevens, K., Gebreyohannes Tewolde, T., Amare, K., Hussein, A., Berhane, G., Baert, R., Ronsse, S.,
917 Kebede, S., Van Hulle, L., Deckers, J., 2015. Water Balance Components for Sustainability
918 Assessment of Groundwater-Dependent Agriculture: Example of the Mendae Plain (Tigray,
919 Ethiopia). L. Degrad. Dev. 26, 725–736.

920 Walraevens, K., Vandecasteele, I., Martens, K., Nyssen, J., Moeyersons, J., Gebreyohannes, T., De Smedt,
921 F., Poesen, J., Deckers, J., Van Camp, M., 2009. Groundwater recharge and flow in a small mountain
922 catchment in northern Ethiopia. Hydrol. Sci. J. 54, 739–753. doi:10.1623/hysj.54.4.739

923 Wang, Z.-M., Batelaan, O., De Smedt, F., 1996. A distributed model for water and energy transfer
924 between soil, plants and atmosphere (WetSpa). Phys. Chem. Earth 21, 189–193.

925 Woldeamlak, S.T., Batelaan, O., De Smedt, F., 2007. Effects of climate change on the groundwater
926 system in the Grote-Nete catchment, Belgium. Hydrogeol. J. 15, 891–901.

927 Zenebe, A., Vanmaercke, M., Poesen, J., Verstraeten, G., Haregeweyn, N., Haile, M., Amare, K., Deckers,
928 J., 2013. Spatial and temporal variability of river flows in the degraded semi-arid tropical mountains
929 of northern Ethiopia 57, 143–169. doi:10.1127/0372-8854/2012/0080

930

- Efficient WetSpa model is developed for the mountainous and semi-arid Geba basin.
- Annual recharge varies from 45 to 208 mm temporally and 0 to 371 mm spatially.
- Recharge strongly related to rainfall; and partly to soil and land-use than other basin physical characteristics.
- ET and soil moisture are annually constant than GW recharge and surface runoff.
- 11.4%, 10%, 94% are recharge, runoff and ET respectively of the precipitation.